

**Review Article****Application of Fluorescence Resonance Energy Transfer in the Clinical Laboratory: Routine and Research****János Szöllősi,\* Sándor Damjanovich, and László Mátyus**

Department of Biophysics and Cell Biology, University Medical School of Debrecen, Debrecen, Hungary

Fluorescence resonance energy transfer (FRET) phenomenon has been applied to a variety of scientific challenges in the past. The potential utility of this biophysical tool will be revisited in the 21st century. The rapid digital signal processing in conjunction with personal computers and the wide use of multicolor laser technology in clinical flow cytometry opened an opportunity for multiplexed assay systems. The concept is very simple. Color-coded microspheres are used as solid-phase matrix for the detection of fluorescent labeled molecules. It is the homogeneous assay methodology in which solid-phase particles behave similarly to the dynamics of a liquid environment. This approach offers a rapid cost-effective technology that harnesses a wide variety of fluorochromes and lasers. With this microsphere technology, the potential applications for clinical flow cytometry in the future are enormous. This new approach of well-established clinically proven methods sets the stage to briefly review the theoretical and practical aspects of FRET technology. The review shows various applications of FRET in research and clinical laboratories. Combination of FRET with monoclonal antibodies resulted in a boom of structural analysis of proteins in solutions and also in biological membranes. Cell surface mapping of cluster of differentiation molecules on immunocompetent cells has gained more and more interest in the last decade. Several examples for biological applications are discussed in detail. FRET can also be used to improve the spectral characteristics of fluorescent dyes and dye combinations, such as the tandem dyes in flow and image cytometry and the FRET primers in DNA sequencing and polymerase chain reactions. The advantages and disadvantages of donor-acceptor dye combinations are evaluated. In addition, the sensitivity of FRET provides the basis for establishing fast, robust, and accurate enzyme assays and immunoassays. Benefits and limitations of FRET-based assays are thoroughly scrutinized. At the end of the paper we review the future of FRET methodology. *Cytometry (Comm. Clin. Cytometry)* 34:159–179, 1998. © 1998 Wiley-Liss, Inc.

**Key terms:** fluorescence resonance energy transfer; tandem dyes; enzyme assay; immunoassays; DNA sequencing; cell surface mapping

Although the phenomenon of fluorescence resonance energy transfer (FRET) was observed by Perrin at the beginning of the century, it was Theodor Förster who proposed a theory describing long-range dipole-dipole interactions between fluorescent molecules approximately 50 years ago (29,30). He derived an equation that relates the transfer rate to the interchromophore and the spectroscopic properties of the chromophores. The ingenious discovery that a fluorescence dipole-dipole interaction, besides orientational and other spectroscopic parameters, which can be kept under control, depends on the negative sixth power of their distance provided one of the most sensitive methods to measure molecular and atomic distance relations at the nanometer level. The utilization of this method in chemistry and biochemistry reached a pinnacle in the 1970s. Cell biological applications also started in the 1970s, but widespread application began only a decade later and is still flourishing.

FRET is widely utilized for a variety of applications. In one series of studies, FRET is used as a tool for ensuring high sensitivity. FRET technology can be incorporated into chromatographic assays, electrophoresis, microscopy, and flow cytometry. FRET also can be used for improving spectral characteristics of fluorescent dyes. In another group of studies, FRET is used to obtain structural information that is otherwise difficult to obtain. The major advantage of applying FRET for structural studies is that

Contract grant sponsor: Hungarian Academy of Sciences; Contract grant numbers: OTKA T019372, T023835, and 6221; Contract grant sponsor: Ministry of Public Health; Contract grant numbers: ETT 344/96 and 359/96; Contract grant sponsor: Ministry of Education; Contract grant number: FKFP 1015/1997.

\*Correspondence to: János Szöllősi, Department of Biophysics and Cell Biology, University Medical School of Debrecen, P.O. Box 39, Nagygyerdei krt. 98, H-4012 Debrecen, Hungary.

E-mail: szollo@jaguar.dote.hu

Received 9 March 1988; Accepted 29 May 1988

owing to the specific labeling the experimental object can be investigated *in situ* and/or *in vivo* with little or no interference regardless of the complexity and heterogeneity of the system.

Although numerous reviews are available on fluorescence resonance energy transfer (17,18,21,28,69–71,90,94,98,100,106–108,127), there is paucity of information regarding the clinical applications of the technology. In this review, an attempt has been made to summarize and describe recent applications of the FRET in routine and research clinical laboratories. The topics and publications discussed in this review undoubtedly reflect the interest of the authors, but we did our best to review relevant literature. First, we describe briefly the theory behind FRET, then the measuring techniques are introduced. Next, papers dealing with the structure and cell surface distribution of cluster of differentiation (CD) molecules are summarized and the analytical applications of FRET are described. At the end of the paper, the future prospects of FRET applications are discussed. The papers reviewed were selected because they had introduced new or improved methods for FRET measurements and analysis or led to a better understanding of important biological structures.

Three directions with enormous clinical potential influenced the selection of reviewed topics in the future. The current interest in quantitative fluorescence determination with simultaneous multicolor immunophenotyping as it applies to clinical immunology. Secondly, the rapidly increasing interest in flow cytometer-based multiplexed immunoassays. This microsphere-based technology revisits the well-characterized solid-phase immunoassays and bioassays that were developed in the 1970s. In the case of the multiplexed solid-phase technology, the epitopes are suspended uniformly in a liquid environment on solid phase (31,73). This paradox-like situation permits harnessing the benefit of both liquid and solid-phase technologies. The novel application is based on rapid identifications of various microsphere populations with subtle differences attributed to spectral emission profiles related to various distinct shades of dyes embedded in their surfaces. The permutations of discrete microsphere types rendered by four-color clinical flow cytometry is staggering. Each color-coded population of microsphere set carries reactants for a distinct bioassay. The solid-phase compartment-based technology opens new doors in unrelated areas, such as pharmacokinetics for drug discovery studies, nucleic acid-based tissue typing, and competitive DNA hybridization, that were not readily available for rapid flow cytometric-based applications in the past. Finally, in the future, the miniaturization of flow cytometric instrumentation will force a new approach to evaluate the relationship between solid phase and liquid phase in the context of rapid immunochemistry. There is a need to revisit the role of transfer rate equation that relates to the interchromophore and the spectroscopic properties of the chromophores. The ultimate exploitation of FRET will come at the end of this century by focusing on the interface between molecular pharmacology and medical chemistry for drug

development. Will flow cytometry have a role in this fascinating scientific challenge?

#### THEORY OF FRET

The theory of FRET was first described by Förster in the late forties, its application to measure distances between donor and acceptor molecules came decades later (20,21,28–30,58,69–71,94,100,106–108). FRET is a radiationless process in which energy is transferred from an excited donor molecule to an acceptor molecule under favorable conditions. One of the most important factors is the distance between the donor and acceptor molecules. Because the rate of energy transfer is inversely proportional to the sixth power of the distance between the donor and acceptor, the energy transfer efficiency is extremely sensitive to distance changes. Energy transfer occurs in the 1- to 10-nm distance range with measurable efficiency, and these distances correlate well with macromolecular dimensions.

Consider a system with two different fluorophores in which the molecule with higher energy absorption is defined as the donor (D) and the one with lower energy absorption is defined as acceptor (A). If the donor is in the excited state, it will lose energy by internal conversion until it reaches the ground vibrational level of the first excited state. If the donor emission energies overlap with the acceptor absorption energies, through weak coupling, the following resonance can occur:



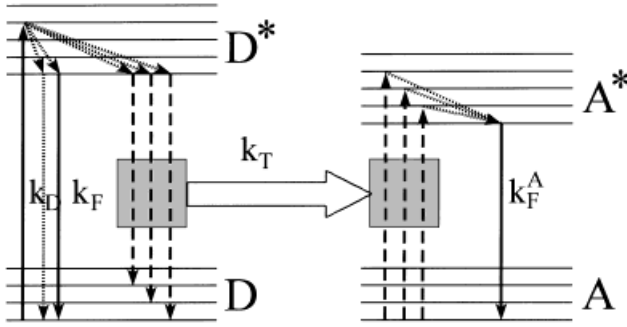
where  $D$  and  $A$  denote the donor and the acceptor molecules in ground state, and  $D^*$  and  $A^*$  denote the first excited states of the fluorophores. The rate of the forward process is  $k_T$  and the rate of the inverse process is  $k_{-T}$ . Because vibrational relaxation converts the excited acceptor into the ground vibrational level, the inverse process is highly unlikely to occur. As a result, the donor molecules become quenched, while the acceptor molecules become excited and, under favorable conditions, can emit fluorescent light. This latter process is called sensitized emission (Fig. 1).

According to the theory of Förster, the rate ( $k_T$ ) and efficiency ( $E$ ) of energy transfer can be written as:

$$k_T = \text{const } J n^{-4} R^{-6} \kappa^2 \quad (2)$$

$$E = \frac{k_T}{k_T + k_f + k_D} \quad (3)$$

where  $k_f$  is the rate constant of fluorescence emission of the donor and  $k_D$  is the sum of the rate constants of all other deexcitation processes of the donor.  $R$  is the separation distance between the donor and acceptor molecules, and  $\kappa^2$  is an orientation factor that is a function of the relative orientation of the donor's emission dipole and the acceptor's absorption dipole. Other parameters are  $n$ , the refractive index of the medium, and  $J$ , the



$$E = k_T / (k_T + k_F + k_D)$$

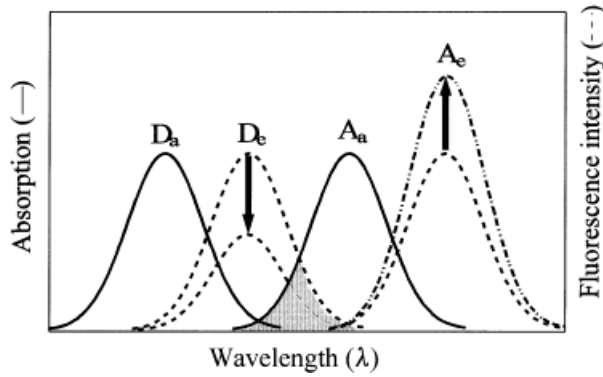


FIG. 1. Energy balance of FRET. The top part of the figure shows the Jablonski energy level diagram. The donor fluorophore is excited and rapidly drops to the lowest vibrational level of the excited state, where it can decay radiatively (fluorescence) or by internal conversion (heat) to the ground state, or transfer energy to the acceptor. Only those levels of the donor and acceptor with similar energies contribute significantly to the transfer rate. Once the acceptor is excited, rapid vibrational relaxation prevents back transfer. The acceptor then decays to the ground state via fluorescence or heat. The bottom part of the figure shows the spectral characteristics and changes of the donor and acceptor undergoing FRET. The donor intensity decreases and the acceptor increases (i.e., is sensitized) with energy transfer. The spectral overlap that makes FRET possible is shown in gray. The absorbance and emission intensities are normalized for display purposes.

spectral overlap integral, which is proportional to the overlap in the emission spectrum of the donor and the absorption spectrum of the acceptor:

$$J = \frac{\int F_D(\lambda) \epsilon_A(\lambda) \lambda^{-4} d\lambda}{\int F_D(\lambda) d(\lambda)} \quad (4)$$

where  $F_D(\lambda)$  is the fluorescence intensity of the donor at wavelength  $\lambda$ ,  $\epsilon_A(\lambda)$  is the molar extinction coefficient of the acceptor.

For dipole-dipole energy transfer it can be shown that:

$$\kappa^2 = (\cos \alpha - 3 \cos \beta \cos \gamma)^2 \quad (5)$$

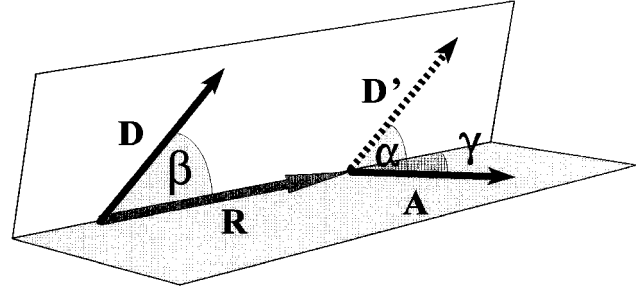


FIG. 2. Orientation of the transition moments of donor and acceptor molecules.  $\alpha$  is the angle between the transition moments,  $\beta$  is the angle between the transition moment of the donor and the line joining the fluorophores, and  $\gamma$  is the angle between the transition moment of the acceptor and the line joining the fluorophores.

where  $\alpha$  is the angle of the transition moments of the donor and the acceptor, and  $\beta$  and  $\gamma$  are the angles between the line joining the centers of the fluorophores and their transition moments (Fig. 2). Uncertainties in the value of  $\kappa^2$  cause the greatest error in distance determination by energy transfer. (Fortunately  $R$  depends on  $(\kappa^2)^{1/6}$ ). The direct measurement of its value is impossible. From theoretical considerations  $\kappa^2$  is in the range between 0 and 4. Assuming random orientation of the donor and the acceptor  $\kappa^2$  becomes 2/3. In the case of cell surface components this assumption is reasonable (19). It can be shown that:

$$E = \frac{R^{-6}}{R^{-6} + R_0^{-6}} \quad (6)$$

From Equations 2 and 3 it follows that:

$$k_T = \frac{1}{\tau} \left( \frac{R_0}{R} \right)^6 \quad (7)$$

where  $\tau$  is the donor's lifetime in the absence of the acceptor, and  $R_0$  is the characteristic distance between the donor and the acceptor when the transfer efficiency is 50%.

$$R_0 = \text{const} (J_K Q_D n^{-4})^{1/6} \quad (8)$$

In this equation,  $Q_D$  is the quantum efficiency of the donor in the absence of the acceptor.

The energy transfer efficiency, as follows from the above formulas, can be determined in a number of different ways. Since energy is transferred from the excited donor to the acceptor, the lifetime ( $\tau$ ), quantum efficiency ( $Q$ ), and fluorescence intensity ( $F$ ) of the donor decrease, if the acceptor is present. As a consequence, the fluorescence intensity of the acceptor increases if the donor is present.

$$1 - E = \frac{\tau_D^A}{\tau_D} \quad (9)$$

$$1 - E = \frac{F_D^A}{F_D} = \frac{Q_D^A}{Q_D} \quad (10)$$

$$\frac{F_A^D}{F_A} = 1 + \left( \frac{\epsilon_D C_D}{\epsilon_A C_A} \right) E \quad (11)$$

In the previous formulas the lower indexes refer to the donor (D) or acceptor (A), whereas the upper indexes indicate the presence of the donor (D) or the acceptor (A) in the system, while  $C_D$  and  $C_A$  are the molar concentrations,  $\epsilon_D$  and  $\epsilon_A$  are the molar absorption coefficients of the donor and the acceptor. Another possibility for determining the energy transfer efficiency is based on the more depolarized emission of the acceptor. Detailed evaluation of the energy transfer measurements can be found in several recent reviews (69–71,100,106,108).

Calculation of distance relationships from energy transfer efficiencies is easy in the case of a single donor single acceptor system if the localization and relative orientation of the fluorophores is known. However, if cell membrane components are investigated, a two dimensional restriction applies for the labeled molecules. Analytical solutions for randomly distributed donor and acceptor molecules and numerical solutions for nonrandom distribution have been elaborated by different groups (24,26,27,35,36, 92,124). In order to differentiate between random and nonrandom distributions, energy transfer efficiencies have to be determined at different acceptor concentrations.

## MEASURING TECHNIQUES

### Spectrofluorimetry

For the case of spectrofluorometric measurements, Equations 10 and 11 are used to determine the energy transfer efficiency. A complete set of samples for transfer efficiency determination should contain at least one unlabeled, two single-labeled (one labeled with donor only and one labeled with acceptor only) and a double-labeled (labeled with donor and acceptor) sample. The measured fluorescence intensities have to be corrected intensities, i.e. for autofluorescence and light scattering. This can be achieved using the unlabeled sample. At the same time the fluorescence intensities should be normalized to the same donor (Equation 10) or acceptor (Equation 11) concentration. For both corrections very accurate sample preparation is required. The dye concentration should be carefully controlled.

In the case of cell suspension another possible error source is the contribution from unbound fluorophores and cell debris to the specific fluorescence. These are very difficult, if not impossible to control, especially if the fluorescent label has a low binding constant. Multiple washing decreases the contribution of free fluorophores to the fluorescence intensity, but unavoidably increases the amount of cell debris. Fluorescence microscopy overcomes most of the problems one faces using spectrofluorometry. The distortion caused by dead cells or cell debris can be avoided, and uncertainties in cell concentration do not cause a problem either. Measurement of energy

transfer in a microscope has the advantage of the spatial resolution, thus providing structural information at the same time. The only disadvantage is statistical accuracy, because only a relatively small number of cells can be investigated.

### Flow Cytometry

Flow cytometry offers a good compromise for both measuring energy transfer on cell surfaces, combining some of the advantages of the spectrofluorometric and microscopic methods. In the case of flow cytometry, the effect of light scattering on fluorescence intensities is practically negligible. Because the receptor densities have great variation in a cell population, normalization of fluorescence intensities on a cell-by-cell basis can not be done using the spectrofluorometric approach. Real single-cell determination of energy transfer requires the measurement of all parameters on the same cell. In flow cytometric measurements there are three unknown parameters: the unquenched donor fluorescence intensity, the nonenhanced acceptor intensity, and the efficiency of the energy transfer. In order to determine these parameters one has to measure three independent signals from the same cell. Two of these parameters are the emission intensities detected from different spectral bands. The third emission intensity is the one resulting from a second exciting laser beam. To this end, a conventional flow cytometer may be modified by the introduction of a second excitation laser beam. The technical details of such a system were described elsewhere (22,100,102,103,109). Briefly, in such a system the 488-nm and the 514-nm lines of an argon ion laser are used for excitation. The laser beams are displaced by about 0.5 mm at the so-called intersection point, where the laser beams illuminate the cells. Spectral ranges of fluorescence are detected around the emission maximum of fluorescein (535 nm) and usually above 590 nm (emission of rhodamine). Data collection is done in list mode, meaning that the corresponding light scatter and fluorescence intensities from each cell are stored separately. The calculation of energy transfer efficiency is done by a computer using Equations 15 and 16. In Equations 12–15, the measured intensities are  $I_1$ ,  $I_2$ , and  $I_3$  and the excitation and emission wavelengths are given in parentheses.  $I_F$  and  $I_R$  stand for the theoretical (unquenched and nonenhanced) intensities of the donor (excited at 488 nm, emission detected at 535 nm) and of the acceptor (excited at 514 nm, detected at >590 nm), respectively. Because the emission spectra of the fluorescein and rhodamine overlap, and both molecules can be excited by the use of both laser beams, correction factors have to be introduced. These factors are  $S_1$ ,  $S_2$ , and  $S_3$ . The definitions of these parameters are as follows:

$$S_1 = I_2/I_1$$

(determined using only donor labeled cells);

$$S_2 = I_2/I_3$$

(determined using only acceptor labeled cells); and

$$S_3 = I_3/I_1$$

(determined using only donor labeled cells).

The three detected intensities can be expressed as

$$I_1(488 \rightarrow 535) = I_F(1 - E) \quad (12)$$

$$I_2(488 \rightarrow >590) = I_F(1 - E)S_1 + I_R S_2 + I_F E \alpha \quad (13)$$

$$I_3(514 \rightarrow >590) = I_F(1 - E)S_3 + I_R + \frac{S_3}{S_1} I_F E \alpha \quad (14)$$

$I_1$  is smaller than  $I_F$  because the energy transfer causes donor quenching.  $I_2$  consists of three additive terms: 1) the overlapping fraction of the quenched fluorescein intensity, 2) the direct contribution of rhodamine, and 3) sensitized emission due to energy transfer. The proportionality factor  $\alpha$  is the ratio of  $I_2$  for a given number of rhodamine molecules and  $I_1$  for the same number of fluorescein molecules.  $\alpha$  is constant for each experimental setup, and has to be determined for every defined case.  $I_3$  is a sum of: 1) a fraction of the quenched fluorescein intensity, 2) the rhodamine intensity, and 3) the sensitized emission of rhodamine due to energy transfer corrected for the lower molar extinction coefficient of fluorescein at 514 nm than at 488 nm.

From Equations 12–14, the following equation can be derived:

$$\frac{E}{1 - E} = \frac{1}{\alpha} \left[ \frac{(I_2 - S_2 I_3)}{\left(1 - \frac{S_3 S_2}{S_1}\right) I_1} - S_1 \right] \quad (15)$$

All the parameters in Equation 15 can be determined experimentally. If we substitute B in the right side of Equation 15, E can be expressed as follows:

$$E = \frac{B}{1 + B} \quad (16)$$

Because fluorescein is used as a donor and rhodamine as an acceptor in most flow cytometric energy transfer experiments, the above considerations apply to them. The equations are valid for other donor acceptor pairs, but the different spectral characteristics must be considered.

In Equations 12–15, it is assumed that the contribution of cellular autofluorescence to the specific fluorescence signals is negligible. If the autofluorescence is substantial, corrections should be done. In this case, however, the correction for autofluorescence can be done using the average autofluorescence intensities of the entire cell population. It should be noted that since in most cell types there is a good correlation between the autofluorescence

detected at different regions of the spectrum, a more elaborate correction method is also possible. Here another independent parameter should be detected, a fourth fluorescence intensity, and this way the autofluorescence can be calculated on a cell-by-cell basis. Naturally high autofluorescence may decrease the precision of the measurements.

## IMAGE CYTOMETRY

### Photobleaching FRET Digital Imaging Microscopy

Jovin and Arndt-Jovin introduced another approach to determine transfer efficiencies in a microscope (47,48). The energy transfer is calculated from the photobleaching kinetics of the donor in the presence and in the absence of the acceptor. Their method is based on the fact that the integrated fluorescence intensity during complete photobleaching is independent from the quantum efficiency of the fluorophore and therefore it is proportional to the donor concentration (41). It is assumed that the donor's photobleaching occurs from the excited singlet state. It can be derived that the energy transfer efficiency can be calculated as follows:

$$E = 1 - \frac{\tau_{ble}}{\tau_{ble}^A} = 1 - \frac{(I_0^A/I_{int}^A)}{(I_0/I_{int})} \quad (17)$$

where  $\tau_{ble}$  is the time constant of photobleaching,  $I_0$  is the initial fluorescence intensity, and  $I_{int}$  is the integrated fluorescence intensity upon complete photobleaching of the donor. The *A* upper indexes indicate the presence of an adequate acceptor. The detailed derivation of the above formula is described in references (47,48). In the case of energy transfer, because there is extra possibility for de-excitation, the availability of excited donors for photobleaching will decrease. As a consequence, the rate of photobleaching will be slower, starting from a quenched initial fluorescence intensity, but the integrated fluorescence intensity remains unchanged.

This method offers a greater sensitivity with an internal control for real donor concentration. The only drawback of the method is the limited number of cells that can be measured. This may cause that inhomogeneities in the sample are not revealed. However, if the same experiment is performed on a flow cytometer this disadvantage can be overcome. Since the introduction of this approach several successful adaptations for different systems have been elaborated (2,95–97).

### Intensity-Based Microscopy

The first semiquantitative intensity-based microscopic method for measuring FRET was introduced approximately 10 years ago (112,113). Uster and Pagano installed an additional filter combination for detecting the “transfer signal” by using the excitation wavelength of the donor and detecting the sensitized emission of the acceptor. This approach is suitable for proving the existence of energy transfer, but the accurate determination of the transfer

efficiency is not possible. More recently, others (83,132) used a similar approach with slight modifications.

In the family of the intensity-based microscopic methods, two relatively new versions emerged. The first (79) uses a set of equations similar to those described by Trón (109), whereas the other calculates corrected ratio images taken from the donor and the acceptor as well (54). Both versions are suitable for determining the transfer efficiencies on pixel basis.

#### APPLICATION OF FRET Research

**Cell surface distribution of hematopoietic cluster of differentiation (CD) molecules.** A nonrandomized codistribution of membrane-bound proteins play an important role in signal transduction across the cell membrane. The primary target for external stimuli is the plasma membrane. In addition to the well-known biochemical mechanisms of ligand-receptor interaction there are numerous physical events that induce alterations of the cell surface in the vicinity of the receptor. Signal transduction is often accompanied by the dynamic rearrangement of the two dimensional patterns of the macromolecular constituents at the cell surface.

The most commonly used methods for determining molecular associations in membranes include cocapping, co-immunoprecipitations, chemical cross-linking, modified fluorescence recovery after photobleaching, electron microscopy, atomic force microscopy, and FRET measurements. Application of one method alone usually does not give a conclusive picture. Results of two or more methods, however, reinforce each other and lead to a consistent picture of the molecular interactions in the plasma membrane. We will focus mostly on results gained by FRET technique, some of the supporting data obtained by other biochemical and biophysical methods will also be mentioned. There have been several general reviews on mapping cell surface elements using FRET technique (17,18,21,70,71,98,108,127); this chapter will focus mainly on the latest results concerning this field.

Although the major histocompatibility complex (MHC) class I and class II molecules are structurally and functionally distinct, there is evidence that MHC class I and class II molecules can be more intimately related than previously thought. It has been reported that MHC class I-specific antibodies can cocap MHC class II antigens on B lymphocytes (77,78). These observations prompted us to perform studies in which a more direct approach, FRET technique, was applied for the investigation of the possible association between HLA class I and class II molecules on PGF and JY B lymphoblastoid cells (99). A panel of monoclonal antibodies specific for various class I and class II antigens was labeled with either FITC (donor) or TRITC (acceptor). Flow cytometric energy transfer measurements were made on cells labeled with fluoresceinated and rhodaminated antibodies simultaneously. FRET efficiency was calculated on a cell-by-cell basis and the results were displayed as energy transfer distribution histograms. Mean values of such distribution histograms were used to draw conclu-

sions about the proximity relationship of cell surface proteins under investigation. This type of FRET study revealed that HLA class I and class II molecules are expressed mostly in a monomeric state on the cell surface. Class II antigens may form heteroassociations among themselves and there is association between class I and class II molecules. There is an equilibrium between free nonassociated HLA class I and class II molecules and the associated class I-class II antigen complexes. The number of class I-class II molecule associations formed depends upon the available class I and class II molecules expressed in the plasma membrane. These results are also in agreement with cocapping experiments demonstrating class I-class II interaction. Our data, however, demonstrated that these complexes are physically associated before cocapping (99). While there was no homoassociation between HLA class I molecules on PGF cells, we could detect homoassociation between them on JY cells. The degree of homoassociation of class I antigens highly depends on the culturing conditions, whether the cells were in log phase or in plateau phase. HLA class I clustering correlated with the expression level of  $\beta_2$ -microglobulin-free HLA class I heavy chains, and the addition of exogenous  $\beta_2$ -microglobulin greatly reduced the HLA class I homoassociation (9). Moreover, modulation of the composition of plasma membrane also influenced the HLA class I clustering. Addition of cholesterol decreased the membrane fluidity and also the degree of homoassociation of HLA class I molecules (9).

We have extended these types of flow cytometric energy transfer measurements and molecular associations have been detected between intercellular adhesion molecule 1 (ICAM-1; CD54), HLA class I heavy chain,  $\beta_2$ -microglobulin, and HLA-DR on the cell surface of JY B lymphoma cells (6). Similar heteroassociations were found in the plasma membrane of HUT-102B2 T lymphoma cells, but the significantly different quantitative data suggested a somewhat different cell surface distribution pattern of the molecules. In this case, interleukin-2 (IL-2) receptor  $\alpha$  subunit (IL-2R $\alpha$ , CD25), was also included in the proximity studies. FRET data suggested that ICAM-1 and/or IL-2R $\alpha$  are closer to the  $\beta_2$ -microglobulin than to heavy chain of the HLA class I complex. In addition, a high degree of homoassociation of ICAM-1 molecules was observed. Heteroassociations involving ICAM-1 molecules may play an important role in antigen presentation, T-cell recognition, cytotoxicity, site-directed lymphokine secretion, and other immunological processes (6).

Flow cytometric energy transfer measurements have also been used to study the topological distribution of transferrin receptor (TfR; CD71) relative to the heavy and light chains of the HLA class I molecules, class II molecules, interleukin receptor  $\alpha$ -chain (CD25), and ICAM-1 (CD54) molecules on HUT-102B2 T and JY B cell lines (72). TfR showed high degree of homoassociation, and its cell surface distribution depended upon the growing condition of cells. TfR was in close vicinity to HLA class I molecules on the surface of JY cells in both logarithmic and plateau phase, whereas it was not associated with HLA

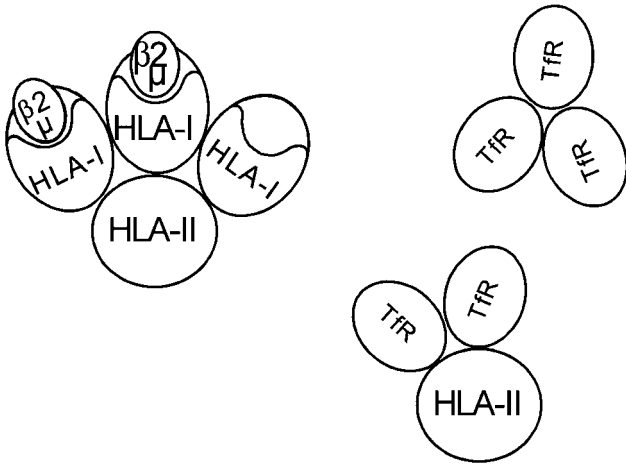


Fig. 3. Schematic representation of the lateral distribution of transferrin receptor (Tfr), HLA class I (HLA I), HLA class II (HLA II) molecules on the surface of JY lymphoblastoid B cells. Note that the transferrin receptor shows high degree of homoassociation and associates with HLA class II molecules but not with HLA class I molecules. The complexes shown are only examples of possible clusters.

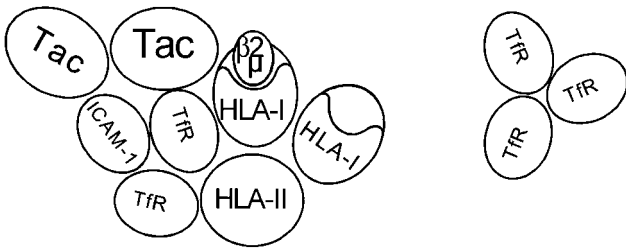


Fig. 4. Schematic representation of the lateral organization of transferrin receptor (Tfr), IL-2 receptor  $\alpha$  chain (Tac), intercellular adhesion molecule-1 (ICAM-1), HLA class I (HLA I), and HLA class II (HLA II) molecules on the surface of HUT-102B2 lymphoblastoid T cells.  $\beta_2$ -microglobulin is the light chain of HLA class I molecule. Note that the transferrin receptor shows high degree of homoassociation and associates with HLA class I, HLA class II, ICAM-1, and Tac. The complexes shown are only examples of possible clusters.

class I on the surface JY cells (Figs. 3 and 4). HLA class II molecules heteroassociated with Tfr on HUT-102B2 cells, whereas only a modest association was found on JY cells, and only in the logarithmic phase (6,72).

Flow cytometric energy transfer measurements have been used to confirm whether coprecipitation of tetraspan molecules (CD37, CD53, CD81, CD82) with HLA class II (DR) antigens is an experimental artefact or reflects real molecular associations in the plasma membrane of live cells. Results of energy transfer experiments carried out with fluorescently labeled monoclonal antibodies (whole antibodies and Fab fragments) demonstrated that the tetraspan molecules are in a single complex with DR molecules rather than each of them is separately associated with different DR molecules (101). The coclustering of these molecules may have functional significance; this is currently under investigation.

Combination of atomic force, electron microscopy, and photobleaching energy transfer made the discovery and

description of the clustering of MHC class I molecules at 2 to 10 nm and also at  $\mu\text{m}$  levels (23). Using flow cytometric and photobleaching energy transfer measurements a non-random distribution pattern of HLA class I molecules was observed in the 2 to 10 nm range. A second, nonrandom, and larger-scale topological organization of the HLA class I molecules was detected by transmission electron microscopy and atomic force microscopy using immunogold labeling. These data suggested that HLA class I antigens exhibit a hierarchical arrangement consisting of specific patterns of localizations but with a degree of randomness in the distribution. The possible function of the higher order clusterization is that by increasing the local density of adhesion molecules and thereby the multiplicity of intercellular interactions, clusters may serve to stabilize weak contacts between cells (23). A similar hierarchical distribution pattern was observed for HLA class II molecules. Electron microscopy also revealed that a fraction of the HLA class II molecules was heteroclustered with HLA class I molecules at the same hierarchical level (46).

CD7 is a 40-kDa glycoprotein that is expressed on a major subset of human peripheral blood T cells. Cross-linking of CD7 monoclonal antibody (mAb) is mitogenic and signals delivered via CD7 molecule stimulated integrin-mediated adhesion (59). Co-immunoprecipitation data suggested that CD7 associate with CD3 and CD45. To confirm this observation, flow cytometric energy transfer measurements were performed using FITC- and TRITC-labeled mAbs as donor acceptor pairs. There was significant increase in the sensitized emission when FITC-CD7 and TRITC-CD45, or FITC-CD7 and TRITC-CD3 interaction was investigated, indicating molecular associations between these entities. These data supported the hypothesis that CD7 exists in an oligomeric complex with CD3/T cell receptor (TCR), CD45, and tyrosine kinase, thereby providing physical basis for the accessory role of the CD7 molecule in T cell activation (59).

Flow cytometric energy transfer measurements were applied to monitor the aggregation of IL-1 type I receptor (CD121a) on transfected C127 mouse mammary carcinoma cells or on Chinese hamster ovary (CHO) cells. Noncompetitive anti-CD121a mAb, M5, was conjugated separately with either FITC (donor) or Cy3 (acceptor) and the cells were labeled simultaneously with a mixture of FITC-M5 and Cy3-M5 antibodies. The ratio of acceptor to donor emission was monitored to detect sensitized emission and donor quenching that occurred upon addition of IL-1 $\alpha$ . FRET results indicated that IL-1 binding led to time-dependent aggregation of IL-1 type I receptor, and that this aggregation is likely to play an important role in IL-1-dependent signal transduction (34).

Vignali and coworkers used also flow cytometry to detect FRET between various domains of CD4 and TCR (114). They used FITC- and TRITC-conjugated mAbs to label specific epitopes on these molecules. CD4 is intimately involved in colocalizing TCR with its specific peptide ligand bound to MHC class II molecules. They wanted to determine which portion and function of CD4 was responsible for the fidelity of the interaction between

TCR and peptide-loaded MHC class II molecules, the distal D1/D2 domains that bind to MHC class II molecules or the membrane proximal D3/D4 domain. FRET data indicated that the D3/D4 domains of CD4 might interact directly or indirectly with the TCR-CD3 complex and influence the signal transduction processes (114).

In contrast to the above-mentioned examples in which mostly flow cytometric energy transfer measurements were used for mapping cell surface distribution of membrane proteins, the application of microscopic energy transfer measurements will be discussed in the following examples. In one article, the photobleaching fluorescence resonance energy transfer (pbFRET) method was applied, in the other paper, intensity-based FRET studies were performed using microscope.

pbFRET technique was used to study the role of CD4 in signal transduction via TCR/CD3 complex. Szabó et al. wanted to reveal whether the inhibition of T cell activation via TCR/CD3 by anti-CD4 antibodies is attributed by the topological separation of CD4-p56/ck from CD3, or by improper apposition (97). The epitopes were liganded with FITC-conjugated antibodies (donor) and PE-conjugated antibodies (acceptor) simultaneously. Results of pbFRET experiments showed that CD4 stayed in the molecular vicinity of CD3, whereas anti-CD3 stimulation was suppressed by anti-CD4 antibodies. Negative signaling via CD4 may be interpreted in terms of functional uncoupling rather than physical separation of CD4 from the TCR/CD3 complex (97).

Jürgens and coworkers also used the pbFRET approach to reveal proximity relationships between the type I receptor for  $F_c\epsilon$  ( $F_c\epsilon$ RI) and the mast cell function-associated antigen (MAFA) (53). Monoclonal antibodies against  $F_c\epsilon$ RI and MAFA were conjugated with FITC (donor) and TRITC (acceptor) whereas the IgE, the ligand for  $F_c\epsilon$ RI, was conjugated with bis(sulfate)-indocarbocyanine Cy3.18-OSu (Cy3) (donor) and bis(sulfate)-indocarbocyanine Cy5.18-OSu (Cy5) (acceptor) and FRET analysis was performed using donor photobleaching digital imaging microscopy. Results of pbFRET analysis suggested that MAFA was in close proximity to at least some of the  $F_c\epsilon$ RI, and clustering of  $F_c\epsilon$ RI leads to no significant change in the proximity of the two molecular species. The association of  $F_c\epsilon$ RI and MAFA establishes a molecular base for MAFA-mediated inhibition of mast cell activation (53).

The best examples for intensity-based FRET measurements were provided by Petty and coworkers. They systematically investigated the interreceptor interactions between  $F_c\gamma$ RIIB (CD16b), a GPI-linked protein, and the leukocyte integrin CR3 ( $\alpha_M\beta_2$ ; CD11b/CD18) (84). They used 3T3 cell lines transfected with either  $F_c\gamma$ RIIB or CR3 or both proteins. Monoclonal antibodies were labeled with FITC and TRITC, and the energy transfer measurements were performed in a microscope. Using appropriate filters and background subtraction FRET signal was detected with a photon counting apparatus. Their results indicated that these two membrane proteins can exist in close physical proximity in membranes and that this association can be affected by an exogenous compound such as *N*-acetyl-D-glucosamine (84). Using the same

resonance energy transfer microscopy approach the group studied the interaction between complement receptor type 3 (CR3) and  $F_c\gamma$ RIIA (CD32). Normal and a tail-minus mutant of  $F_c\gamma$ RIIA were transfected into fibroblasts that did or did not express CR3. Physical proximity was detected between CR3 and  $F_c\gamma$ RIIA on the cell surfaces. Cells expressing only the tail-minus mutant of  $F_c\gamma$ RIIA were unable to internalize opsonized erythrocytes but showed significant binding ability. In contrast, cells expressing both mutant  $F_c\gamma$ RIIA and C3 internalized opsonized erythrocytes. Results showed that CR3 could complement the phagocytic function of defective  $F_c\gamma$ RII (126). FRET microscopy was used to image the spatial distribution of energy transfer efficiency and to follow the kinetics of the association and dissociation of CR3 and the urokinase-type plasminogen activator receptor (uPAR; CD87), a GPI-linked protein. Initial level of FRET dramatically fell during cell polarization, but did not change on cells fixed with paraformaldehyde. This means that interreceptor associations correlate well with cell activity: CR3 and uPAR are coclustered on stationary cells and uncoupled on polarized cells initiating locomotion (56). CD14, another GPI-linked membrane protein, also affected the cell surface distribution of CR3. When cells were treated with endotoxin LPS, which binds CD14, formation of CD14-CR3 complex was initiated. Kinetic studies showed that CD14-CR3 complexes dissociate as neutrophils attach to substrate (129).

**Conformation of membrane proteins.** In addition to the cell surface distribution of membrane proteins the conformation of these molecules can also be investigated by FRET technique. In one approach reactive groups of a protein under investigation are labeled with fluorescent probes, i.e., with donor acceptor pairs, and the variation in FRET efficiency is used to characterize altered conformation of the protein molecule. In the other approach various epitopes of a membrane protein can be labeled with appropriately conjugated monoclonal antibodies or Fab fragments and the change in the intramolecular FRET efficiency is monitored during various treatments.

Zheng et al. have chosen the first approach in order to monitor conformations of IgE bound to its receptor  $F_c\epsilon$ RI and in solution (131). They prepared a mutant IgE ( $\epsilon/C\gamma 3^*$ ) that has a cysteine replacing a serine near the C-terminal end of the heavy chain. This sulfhydryl group was selectively labeled with fluorescein-5-maleimide serving as donor, and the 5-(dimethylamino)naphthalene-1-sulfonyl (DNS) bound to the antigen binding site of the IgE served as acceptor. The resonance energy transfer between these groups was monitored by spectrofluorometry and the average end-to-end distances for IgE in solution and on membranes after forming receptor-IgE complex were compared. These distance measurements clearly demonstrated a bent conformation for IgE bound to its receptor on the cell membrane and also provided evidence for a surprisingly similar conformation for IgE in solution (131).

In contrast to the antibodies, T cells do not recognize antigens in their native conformation, but only after partial proteolysis within antigen processing and presenting cells

into constituent peptides that are then bound to MHC molecules. The bimolecular complex of antigen peptide and MHC molecule is then displayed on the surface of antigen presenting cells and recognized by T cell clones bearing antigen receptor specific for it. MHC class I molecules primarily specialized to present peptide derived from endogenous proteins whereas class II molecules present peptides derived from endocytosed antigens. Tampé and coworkers wanted to address the question of whether MHC class II molecules can bind one or two peptides (105). They compared the peptide binding capacity of the "floppy" and "compact" forms of MHC class II molecules. The floppy conformation is an intermediate in the dissociation of compact into separate  $\alpha$  and  $\beta$  chains. A 170 amino acid peptide from chicken ovalbumin was labeled with fluorescein at the amino terminus or with Texas Red (TR) near the carboxyl terminus. Systematic, spectrofluorometric FRET measurements between fluorescein- and TR-labeled peptides revealed that two full-length peptides can bind to the floppy  $\alpha\beta$  heterodimer, and two truncated peptides can bind to the compact  $\alpha\beta$  heterodimer and also to floppy  $\alpha\beta$  heterodimer. No simultaneous binding of the two full-length peptides to the compact  $\alpha\beta$  conformation was detected. The biological significance of the above-mentioned findings may be that they suggest a mechanism or peptide exchange in class II antigen (105).

Catipovic and coworkers compared the conformation of empty and peptide-loaded MHC class I molecules (11) using flow cytometric FRET measurements. Fluoresceinated Fab fragments of monoclonal antibody specific for  $\alpha 2$  domain of the heavy chain served as donor, and TR-conjugated Fab fragment of monoclonal antibody specific to  $\beta_2$ -microglobulin as acceptor. No FRET was found between empty MHC class I complex, but FRET was detected when the complex was loaded with peptides. These data indicated that empty MHC class I molecules have a flexible and extended conformation that is accessible by peptides. Upon peptide binding, MHC class I molecules adopt a more compact conformation. Because the amount of FRET depends on the sequence of the bound peptide, it appears that this compact MHC conformation is influenced by the peptide (11).

Fluoresceinated and rhodaminated, noncompeting mAbs, which bind to the same H-2K<sup>k</sup> antigen but to different epitopes, were applied to label the surface of HK 22 murine T lymphoma cells. Using flow cytometric technique, significant FRET efficiency was detected between FITC-labeled 30/6 and TRITC-labeled 27/55 antibody because it would be expected for intramolecular transfer efficiency. Addition of specific peptide to the double-labeled cells increased the FRET efficiency significantly. At the same time addition of the specific peptide had no effect on the monomeric state of H-2K<sup>k</sup> molecules. Because a large portion of the MHC class I antigens expressed on the cell surface is already occupied by endogenous peptides the increase in FRET efficiency upon addition of exogenous peptide can be interpreted in the following ways. Addition of peptide induces a huge conformational change in formerly free MHC class I molecules, which can

be 10% to 30% of the total class I molecules. Another possibility is that exogenously added peptides replace almost all the endogenous peptides, and due to its different structure induces a slight conformational change on all class I molecules (98).

Flow cytometric FRET measurements were performed to detect reversible conformational changes in the MHC class I complex in the plasma membrane of JY cells upon depolarization of the transmembrane potential (7). The heavy chain of the MHC class I molecules was labeled with fluoresceinated mAb, while the  $\beta_2$ -microglobulin with rhodaminated mAb. Reduction of transmembrane potential increase the intramolecular FRET efficiency between these antibodies (Fig. 5). Repolarization of the depolarized samples restored the energy transfer efficiency to the original values measured before depolarization. Depolarization caused similar relative changes in FRET efficiency when Fab fragment was used for labeling MHC class I complex, suggesting that the observed phenomenon is not restricted to whole antibodies (7). The magnitude of the conformational change was similar to that observed in MHC class I complex upon specific peptide binding (98). This finding suggested that peptides presenting MHC class I molecules might alter their conformation upon transmembrane potential changes to such an extent that antigen presentation and, thus, cell-mediated cytotoxicity may be influenced. Toward this end, the same group studied the effect of membrane potential changes of target cells on the function of cytotoxic T lymphocytes. Alterations of the resting potential of target cells in both directions resulted in enhanced cytotoxic activity (3). These observations suggested the alteration of membrane potential could directly influence the conformation of proteins critical for immune recognition.

#### Analytical Applications

**Tandem fluorescence dyes in immunophenotyping.** The detection of multiple fluorescent biomarkers on a single cell by flow cytometry provides a powerful tool for cell analysis. Therefore, there is always a need for more fluorophores that can be used simultaneously in immunofluorescence applications. Because most clinical flow cytometers utilize single-laser excitation, conventional low molecular weight fluorescent dyes having small Stokes shift can not be used for the detection of more than two fluorescent parameters on a single cell. The introduction of the phycobiliprotein-based tandem dyes has significantly enhanced the capabilities of these single-laser flow cytometers for performing multiparametric analysis (5,60,86,115). R-PE, a protein of molecular weight 240 kDa containing 34 bilin fluorophores (80) can be applied simultaneously with fluorescein because both can be excited at 488 nm and the PE emission at 575 nm and fluorescein emission at 525 nm can readily be discriminated with optical band-pass interference filters. In addition, PE can be used as energy donor due to its high molar absorption coefficient between 450 and 550 nm, with a range of potential acceptor molecules possessing favorable spectral overlap, including TR, Allophycocyanine

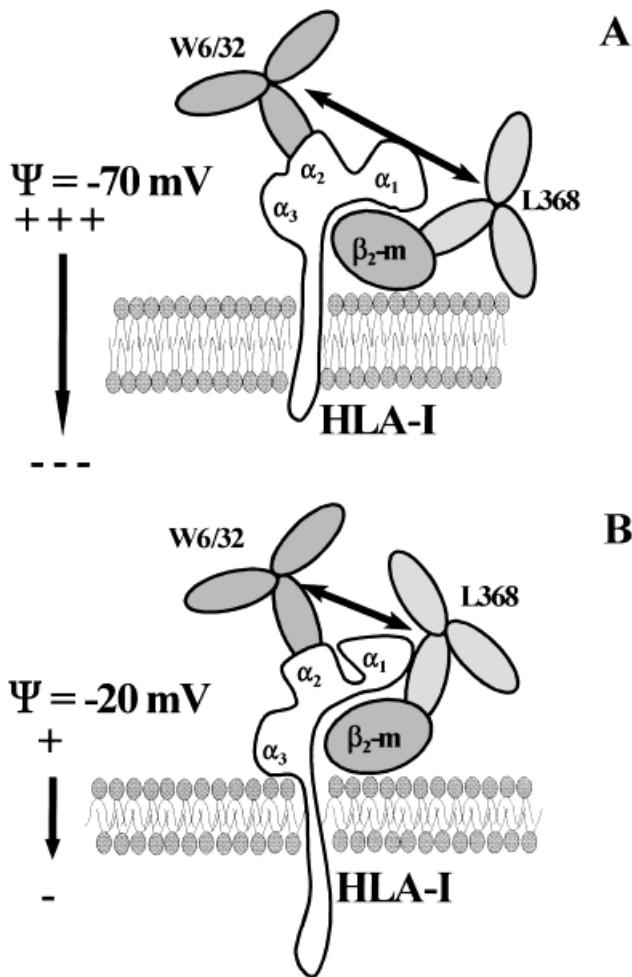


Fig. 5. Schematic representation of HLA class I complex labeled with noncompeting fluorescently tagged antibodies bound to the same complex but to different epitopes. Monoclonal antibody W6/32 binds to the heavy ( $\alpha$ ) chain of the HLA I complex, while L368 to the light chain ( $\beta_2$ -microglobulin) of the complex. Depolarization of the membrane results in conformational change of the HLA class I molecule bringing the tagged epitopes closer to each other.

(APC), and cyanine dyes (Cy5 or Cy7). The Texas Red-PE tandem conjugates have been commercially available under the following trademarks: Duochrome (Becton Dickinson Immunocytometry Systems, Belgium), ECD (Beckman Coulter) and Red 613 (Life Technologies, Rockville, MD). The large Stokes shift associated with the fluorescence resonance energy transfer of these tandems produces emission that can easily be resolved from direct PE or fluorescein emissions. The PE-TR tandem emits at 613 nm, the APC-PE and Cy5-PE at 660–670 nm, and the Cy7-PE at 780 nm, respectively (60,86,115). The largest Stokes shift of 300 nm is provided by the Cy7-PE conjugate that can be efficiently excited at 488 nm and emits at 780 nm. The Cy5-PE and Cy7-PE tandems are very bright fluorescent reagents and can be used with fluorescein and PE with excitation from a single laser light (488 nm) providing a useful fluorophore set for four-color immunofluorescence (86).

Development of tandem reagents is more difficult than development of simple fluorophores primarily because of the added variable: the acceptor-to-donor molar ratio (A/D). In general, a high A/D ratio yields the best transfer efficiency, however, at such ratios the acceptor often self-quenches (producing less fluorescence) and may cause the tandem to become “sticky.” In such an event, the monoclonal antibody-tandem conjugate loses its specificity. Therefore, compromise between optimal transfer efficiency (i.e., low or no direct emission of the PE should be present) and optimal acceptor fluorescence is necessary. In the case of Cy5-PE tandem less Cy5 is needed to quench the direct PE fluorescence than in the case of Cy7-PE conjugate because the spectral overlap between PE and Cy5 is larger than between PE and Cy7 (60,86). Self-quenching due to acceptor dimerization starts above 5 Cy5/PE ratio for Cy5-PE conjugate and above 3 Cy7/PE ratio for Cy7-PE conjugate. Interestingly, the stickiness is much less of a problem for Cy7-PE than for Cy5-PE, which has nonspecific staining when applied to peripheral blood mononuclear cells. It has been suggested that human monocytes might have a “Cy5” receptor resulting in high background binding of Cy5-PE. Cy7-PE conjugated nonrelevant antibodies do not show nonspecific binding on monocytes (86). Although these tandem dyes are very useful in single-laser flow cytometry, not all of them can be utilized for dual-laser application, because the second laser might directly excite the acceptor molecule of the energy transfer pair. For example, in a flow cytometer in which the second laser emits at 633 nm, the application of Cy5-PE tandem dye as a third color on the first laser beam (488 nm) may not be effective. Cy5-PE is efficiently excited with the second laser and, unfortunately, it emits energy in the same region as APC. The exploitation of the second laser beam has been greatly enhanced with the introduction of tandem dyes that work in the red and far-red region (5,86). The other motivation in the development of the red excitable tandem dyes was the challenge to avoid fluorescence near or at cellular autofluorescence, which is often a limiting factor in signal detection. Competition with autofluorescence is much less of a problem when the dye selected is in the red and far-red region. Cy7 dye with its 780-nm emission is a good candidate as a fluorescent probe for flow cytometry, however, the 744-nm excitation is usually unavailable on standard dual-laser flow cytometers. Conjugation of Cy7 to APC resulted in a new tandem construct, the Cy7-APC or ALLO-7 (5,86). The sensitivity of photomultiplier tubes in the 700 to 800 nm region should be increased in order to obtain wider applications of this red tandem dye. ALLO-7 has the potential to increase and diversify the combinations of fluorochromes used with conventional flow cytometers.

The tandem dyes discussed above are bright fluorophores and can easily be coupled to mAbs. These reagents are well suited for a variety of fluorescence applications, including multilaser clinical flow cytometry and microscopy.

**Enzyme assays.** Usually this type of FRET measurement involving synthesized oligomers is not of concern to

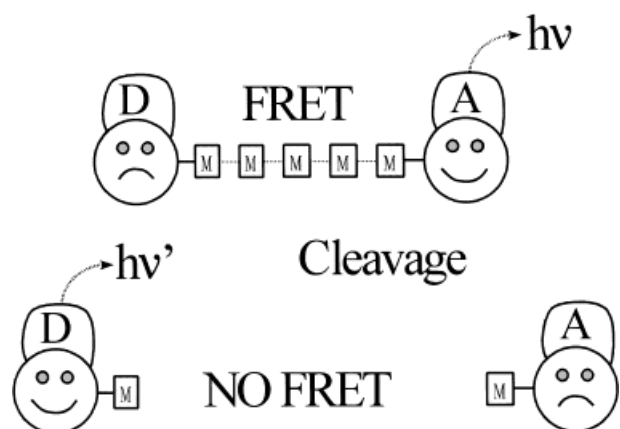


FIG. 6. Enzyme assays based on FRET principle. Fluorogenic substrates are synthesized in which donor and acceptor molecules are attached to monomers (e.g., amino acids, saccharides, nucleotides) and located within the FRET distance. Upon cleavage, the FRET efficiency drops to zero, the intensity of donor increases and the intensity of acceptor decreases.

clinical immunologists. However, the current interest in multiplexed flow cytometric analysis provides an opportunity to revisit some of the classical assay systems involving fluorophores and solid-phase binding. The distance between the locations of the donor and acceptor molecules is of great concern in this type of flow cytometric assay because many analytes form complexes in close proximity to each other. Utilizing microspheres suspended in a liquid medium attached to oligomers with and without fluorescent label sets the stage for a new approach to homogeneous assay systems.

The general scheme of a FRET-based enzyme assay is the following: Oligomer substrates are synthesized that are double labeled with donor and acceptor fluorophores. Usually the distance between the locations of the donor and acceptor molecules is less than  $R_0$ , so the donor fluorescence is significantly quenched in this double conjugate. This intramolecular quenching is relieved by the action of an enzyme that cleaves the oligomer substrate, thereby releasing the donor and acceptor moieties separately into the solution, resulting in tremendous increase in donor fluorescence (Fig. 6). These fluorometric assays are widely used because they provide high sensitivity and the assay can easily be automated.

Proteases are among the most often assayed enzymes. Matayoshi and coworkers have developed a new fluorogenic substrate for assaying retroviral proteases using the FRET principle (66). The assayed enzyme, the 11-kDa protease (PR) encoded with human immunodeficiency virus (HIV) 1, is essential for the correct processing of viral polyproteins. The maturation of infectious virus is therefore a target for the design of selective HIV disease therapeutics. The assay used the quenched fluorogenic substrate 4-[[4'-(dimethylamino)-phenyl]azo]benzoic acid (DABCYL)-Ser-Gln-Asn-Tyr-Pro-Ile-Val-Gln-5-[(2'-aminoethyl)amino]naphthalene-1-sulfonic acid (EDANS), whose peptide sequence was derived from a natural processing site

for HIV-1 PR. The fluorogenic peptide is cleaved at the Tyr-Pro bond resulting in a 40-fold increase in the fluorescence quantum yield. Application of this assay facilitates the identification of novel inhibitors of HIV-1 PR, and permits detailed studies on the activity and inhibition of this enzyme. Because of its simplicity, speed, sensitivity, and precision in kinetic analyses, this method is superior to the more commonly used high-performance liquid chromatography or electrophoresis-based assays for peptide substrate hydrolysis by retroviral PR (66).

The serine protease involved in spreading of an other infectious virus, hepatitis C, is contained within the N-terminal region of nonstructural protein 3 (NS3 protease) and is among the possible targets for therapeutic intervention. Taliani and coworkers also used the above-mentioned DABCYL-EDANS pair to design a fluorogenic substrate for NS3 protease, however, *in vitro* characterization of synthetic substrates based on all of the natural cleavage sites has consistently revealed poor kinetic parameters, making them unsuitable for sensitive high-throughput screening (104). Instead, they have developed a decapeptide substrate incorporating an ester bond within the molecule containing the two fluorophores. With the help of this new substrate a continuous assay for NS3 protease activity was developed, and the detection limit for NS3 was estimated between 1 nM and 250 pM (104).

Wang and coworkers used the same DABCYL-EDANS donor-acceptor pair to design a fluorogenic substrate for continuous assay of renin activity (116). Human renin, an aspartic protease, is one of the most specific proteases and plays an important role in the regulation of blood pressure and in electrolyte homeostasis. The DABCYL-gaba-Ile-His-Pro-Phe-His-Leu-Val-Ile-His-Thr-EDANS substrate incorporates the renin cleavage site that occurs in the N-terminal peptide of human angiotensinogen. The cleavage of the substrate occurs specifically at the Leu-Val bond, which corresponds to the renin cleavage site of angiotensinogen, and leads to a time-dependent increase in fluorescence intensity. It was estimated that with extended incubation time (2 to 3 h) the assay can detect renin at 0.5 ng/ml concentration. The automated, high-throughput fluorometric renin assay version for the 96-well microtiter-plate fluorescence reader is useful for studying enzyme inhibitors and enzyme stability (116).

The DABCYL-EDANS pair proved to be also very useful in developing fluorogenic substrate for interleukin-1 $\beta$  (IL-1 $\beta$ )-converting enzyme (ICE) (82). ICE is a heterodimeric cysteine protease that catalyzes the conversion of the inactive 33-kDa or 31-kDa IL-1 $\beta$  precursor to the 17.5-kDa mature biologically active molecule. The unique cleavage site appears to be conserved in all known IL-1 $\beta$  molecules and occurs between Asp 116 and Ala 117. Upon cleavage of the newly developed DABCYL-Tyr-Val-Ala-Asp-Ala-Pro-Val-EDANS substrate, an increase in fluorescence intensity is observed, permitting continuous assay of ICE. Besides characterizing the enzyme activity of ICE, this assay is useful in screening inhibitory compounds (82).

Another protease, the stromelysin is a member of the matrix metalloproteinase family of enzymes and has been

implicated in the pathogenesis of tumor metastasis and inflammatory diseases such as rheumatoid arthritis. To screen prospective inhibitors of this protease, Bickett and coworkers developed a fluorogenic substrate with excitation and emission spectra compatible with commercially available 96-well plate readers (8). The substrate is based on conjugation of 6[N-(7-nitrobenz-2-oxa-1,3-diazol-4-yl amino) hexanoic acid (NBD) (excitation: 467 nm; emission: 534 nm) and 7-dimethylaminocoumarin-4-acetate (DMC) (excitation: 368 nm; emission: 465 nm) to a peptide substrate for stromelysin. The new substrate NBD-Arg-Pro-Lys-Pro-Leu-Ala-Nva-TRP-Lys-(DMC)-NH<sub>2</sub> is 95% quenched and the fluorescent product Nva-TRP-Lys-(DMC)-NH<sub>2</sub> is easily detected at 368 nm excitation and 465 nm emission. Because of the action of the enzyme, a 20-fold increase in the fluorescence quantum yield can be observed. These characteristics make this compound an excellent substrate for routine determination of in vitro activities of stromelysin inhibitors (8).

Goudreau and coworkers synthesized a novel fluorogenic substrate, dansyl-Gly-(*p*-NO<sub>2</sub>)Phe-βAla, as a selective substrate for neutral endopeptidase 24.11, found on the surface of various cells and involved in processes as diverse as hypertension and the control of vasoactive peptides (33). The neutral endopeptidase also behaves as a lymphocyte marker and is identical to the common acute lymphocytic leukemia antigen (CALLA; CD10). Cleavage of the substrate Gly-(*p*-NO<sub>2</sub>)Phe amide bond leads to an increase in fluorescence related to the disappearance of the intramolecular energy transfer between the dansyl and the nitrophenyl residues. The substrate has advantages over the commercially available dansyl-D-Ala-Gly-(*p*-NO<sub>2</sub>)Phe-Gly, because the Gly residue in the fourth position has been replaced by β-alanine. This increases the selectivity of the substrate for neutral endopeptidase via eliminating a residual sensitivity of the peptide toward angiotensin converting enzyme. In addition, deletion of the D-Ala residue in the second position resulted in an increase in the quenching efficiency, thus raising the sensitivity of the assay (33).

In another set of fluorogenic substrates, only one extrinsic fluorophore is added to the polypeptide chain, because the Trp is used as intrinsic fluorophore in creating the donor/acceptor pair for FRET-based analysis. Stack and Gray designed a fluorogenic substrate for vertebrate collagenase and gelatinase, dinitrophenyl-Pro-Leu-Gly-Leu-Trp-Ala-D-Arg-NH<sub>2</sub> (93). Tryptophan fluorescence was efficiently quenched by the NH<sub>2</sub>-terminal dinitrophenyl group. Increased fluorescence accompanied hydrolysis of the peptide by collagenase or gelatinase. Amino acid analysis of the two-product peptides showed that collagenase and gelatinase cleaved the substrate at the Gly-Leu bond. The specificity of the substrate was also proven by the fact that soluble type I collagen was a competitive inhibitor of peptide hydrolysis by collagenase (93). In the other substrate, designed by Bouvier et al. (10), the indole fluorescence of the tryptophan residue was quenched by an N-terminal dansyl group located five amino acid residues away. The heptapeptide substrate, dansyl-Ala-Tyr-Leu-

Lys-Lys-Trp-Val-NH<sub>2</sub>, is a specific substrate for the promastigote surface protease (PSP) of *Leishmania*. The fluorescent oligopeptide substrate was cleaved by the PSP between the tyrosine and leucine residues and the hydrolysis resulted in a time-dependent increase in fluorescence intensity of 3- to 7-fold. Wang and Liang described a new approach for synthesizing fluorogenic substrates containing only α-amino acids for renin, by incorporating tryptophan and *p*-nitrophenylalanine into peptides (117). In this manner, the substrates can be prepared on a peptide synthesizer, and both ends of these peptides are free; other residues can be attached to increase their solubilities or to label them with affinity ligands. They tested the applicability of this new approach by developing a continuous assay for renin. Hydrolysis of the peptide specific to renin resulted in a 4.5-fold increase in tryptophan fluorescence, suggesting that *p*-nitrophenylalanine quenches about 78% of the fluorescence of tryptophan in this peptide (117).

Not only proteases but also other enzymes have been assayed using FRET-based fluorogenic substrates. For example, introduction of bifluorescent-labeled substrates for endo-type carbohydrases provided a continuous, homogeneous assay for glycoamidases and ceramide glycanases. Earlier, the activity of these enzymes was measured in assays involving the separation of the products. Lee and coworkers prepared a doubly fluorescence-labeled biantennary glycopeptide for glycoamidases and an alkyl lactoside for ceramide glycanases (61). For the glycopeptide substrate, dansyl group (donor) is attached to the terminal galactose and naphthyl group (acceptor) is placed on the N-terminal amino acid. For the alkyl lactoside substrate dansyl group is attached to the omega-amino group of the alkyl aglycon and naphthyl group is attached to the 6'-hydroxyl of lactose. The fluorescence emission of the naphthyl increased as glycoamidase or ceramide glycanase hydrolyzed their respective substrates. Using these substrates, sensitive and convenient assays of these enzymes were established (61). Armand and coworkers synthesized a bifunctionalized tetrasaccharide a substrate to study cellulases, which are usually classified as endoglucanases and cellobiohydrolases (1). The substrate, which carries a 5-(2-aminoethylamino)-1-naphthalenesulfonate group on the nonreducing end and an indolethyl group on the reducing end, could be of general use to measure the kinetic constants of cellulases able to act on oligomers of degree of polymerization less than 5. Their data also proved that cellobiohydrolases I and II are able to degrade an oligosaccharide substrate carrying noncarbohydrate substituents at both ends (1).

Retroviruses require viral DNA to be synthesized by reverse transcription in the cytoplasm followed by integration of the resulting viral DNA into the host chromosome in the nucleus. Reverse transcription and integration, essential steps in the life cycle of retroviruses, are possible targets in the development of antiviral reagents. One attractive target is the integrase protein, a product of the retroviral *pol* gene, which is solely responsible for the retroviral integration process through cutting and joining

reactions. For screening of large numbers of antiviral agents a rapid and precise assay, based on the FRET principle, has been developed (62). Oligonucleotide containing the terminal sequence of HIV-1 DNA and FITC (donor) and EITC (acceptor) were synthesized and annealed to form a fluorogenic substrate for HIV integrase. The authors were able to overcome the problem of earlier attempts in which the fluorophores interacted with the DNA causing quenched fluorescence even after cleavage, via applying a nucleotide analog with a 12-carbon linked arm, 5 amino (12)-2'-deoxyuridine  $\beta$ -cyanoethyl phosphoramidite. The fluorogenic substrate-based assay was standardized with radioactive DNA cleavage reaction. The advantages of the fluorescent assay over the other assays include its speed, continuity of reaction monitoring, sensitivity, specificity, and capacity for automation through a 96-well fluorescence microplate reader (62).

Ghosh and coworkers developed a FRET-based assay for monitoring the kinetics of *PaeR7* endonuclease enzyme activity (32). The authors synthesized a series of duplex substrates with an internal CTCGAG *PaeR7* recognition site and donor (fluorescein) and acceptor (rhodamine) dyes conjugated to the opposing 5' termini applying a 6 mer carbon spacer. Restriction cleavage of the fluorogenic substrate resulted in time-dependent increase in donor fluorescence. The steady state kinetic parameters for these substrates were in agreement with the rate constants obtained from a gel electrophoresis-based fixed time point assay using radiolabeled substrates. The FRET-based method provides a rapid continuous assay as well as high sensitivity and reproducibility (32).

Ribonucleases (Rnases) have also been assayed using fluorogenic substrate. Zelenko and coworkers synthesized DUPAAA, a novel fluorogenic substrate for pancreatic Rnases (130). It consists of the dinucleotide uridylyl-3',5'-deoxyadenosine to which a fluorophore, *o*-aminobenzoic acid, and a quencher, 2,4-dinitroaniline, have been attached by means of phosphodiester linkages. Cleavage of the phosphodiester bond at the 3'-side of the uridylyl residue by RNase caused a 60-fold increase in fluorescence. The substrate was hydrolyzed efficiently by pancreatic Rnases, but no cleavage was observed with the microbial RNase T1 (130).

Luminescence from lanthanides has also been used in FRET-based enzyme assay (16). The lanthanides binds to a mutant  $\text{Ca}^{2+}$  binding protein, oncomodulin, in which salicylic acid is conjugated to a cysteine residue. Luminescence of  $\text{Tb}^{3+}$  resulting from energy transfer from the salicylic group continuously decreased as it was monitored using time resolved luminescence in the presence of proteolytic enzymes such as subtilisin, chymotrypsin, cathepsin B, and HIV-1 protease. The simplicity of the assay coupled with its high level of sensitivity makes it useful for the detection of proteases at very low concentrations (16).

All the above fluorogenic substrates can be applied in vitro. Mitra and coworkers introduced a novel fluorogenic substrate that can be applied for monitoring protease activity within a cell, based on genetic engineering of the

green fluorescent protein (GFP) (74). They fused the C terminus of a red-shifted variant of GFP (RSGFP4) to a flexible polypeptide linker containing a factor Xa protease cleavage site. The C terminus of this linker was fused to the N terminus of a blue variant of GFP (BFP5). The RSGFP4-BFP5 concatamer was cleaved with factor Xa resulting in marked decrease in energy transfer, i.e., increase in donor fluorescence. Although this substrate was tested only in vitro, the authors suggested that this concatamer might have advantages over other methods of monitoring protease activity or screening for protease inhibitors because the assay could be carried out in living cells and in real time. Towards this end cells should be cotransfected with the gene for the protease of interest and the gene for the BFP:RSGFRP concatmer. An intracellular assay may be particularly useful for finding protease inhibitors because factors such as the cytotoxicity of a potential inhibitor and its ability to enter into the cell are automatically determined when screening with this assay.

**Immunoassays.** Interest in measuring the binding interactions between antibodies and their specific antigens has resulted in the application of a broad array of technologies to the development of immunodiagnosics. Fluorescence immunoassays have received considerable attention recently due to their high sensitivity (25,75). Such immunoassays are divided into two categories, heterogeneous assays, which involve physical separation of the assay mixture before detection, and homogeneous assay, in which no separation steps are required. The majority of existing fluoroimmunoassays are heterogeneous. Furthermore, they are often competitive assays in which a fluorescently labeled antigen (or antibody) competes for binding with an unlabeled antigen (or antibody). In such an assay, the fluorescently labeled species are referred to as the tracer, and the unlabeled species as the analyte. Depending on the assay being performed, the analyte can be either an antigen (Ag) or an antibody (Ab). After removal of unbound analyte and tracer, the signal intensity from the bound tracer is found to be inversely proportional to the analyte concentration in the original solutions. The separation step always complicates the design of immunoassays and can degrade their overall performance.

Consequently, homogeneous immunoassays are advantageous because they are conducted entirely in the original sample mixture, requiring fewer manipulations, rendering the assay for easy automation. In general this results in fewer sources of imprecision, shorter times to results and decreased hazards due to sample handling. Homogeneous immunofluorescence assays can be based on several types of physicochemical interactions. They modulate the label emission within the immunological complex (39), including spectral changes of a fluorescent labeled antibody upon binding of unlabeled Ag (63). Changes may arise in fluorescence polarization and fluorescence lifetime during assay reaction (38,40), and in FRET processes brought about during immune complex formation (110).

Ullman et al. (111) in 1976 developed the first immunoassay based on FRET. They applied fluorescein labeled

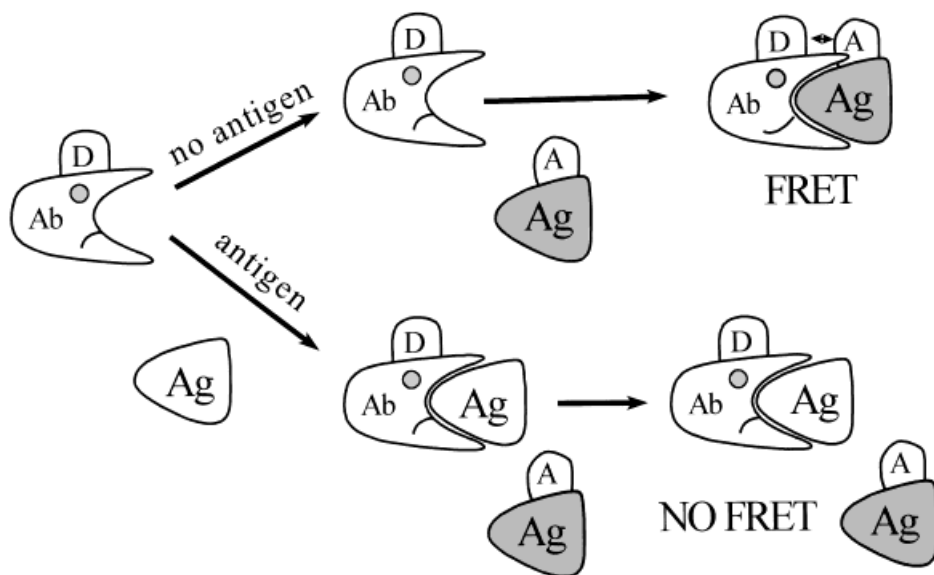


FIG. 7. FRET-based homogeneous, competitive immunoassay. Antibodies and antigens are labeled with donor and acceptor molecules respectively. The analyte is the unlabeled antigen in this competitive assay. The extent of quenching (FRET) decreases in the presence of the unlabeled antigen.

antigen as donor and rhodamine labeled antibody as acceptor. The size of the antigen and antibody complex was compatible with the FRET distance, thus the complex led to fluorescence quenching. Inclusion of unlabeled antigen reduced the available binding sites by competitive binding thus reducing the amount of quenching (Fig. 7).

In the second approach, separate portions of antibody were labeled with fluorescein and rhodamine, respectively. Provided that multivalent antigen is used, admixture of the differently labeled antibody fractions with unlabeled antigen should reduce the fluorescence intensity by bringing the donor and acceptor within close proximity (Fig. 8). The first approach was applied successfully for detection of fluorescein-labeled morphine conjugates in the 100 pM range and above. In the second approach morphine-albumin conjugate was used as multivalent antigen and up to 20 anti-morphine antibody was able to bind to morphine-albumin conjugate (111).

Thorough analysis of the optimal conditions of this FRET-based immunoassay system revealed that although fluorescein and rhodamine as the donor and acceptor labels are perfectly practicable, these fluorophores are by no means ideal for use in such an assay (64,110). Particular disadvantages include the poor stability of rhodamine-labeled antibodies, and the overlap of fluorescein and rhodamine absorption spectra. In addition, the Stokes shift for fluorescein is relatively small, so interference from scattered light may limit the sensitivity of the assay in biological samples. Usually the intensity of rhodamine emission at 580 nm is too feeble to permit its routine use in an assay based on fluorescence sensitization (64,110).

To overcome some of the above-mentioned problems, 4',5'-dimethoxy-6-carboxyfluorescein was introduced as a new acceptor in FRET-based immunoassay (55). This compound is nonfluorescent and participates in "dark" transfer process, giving no contribution to the background fluorescence of the assay mixture. In addition, due to the

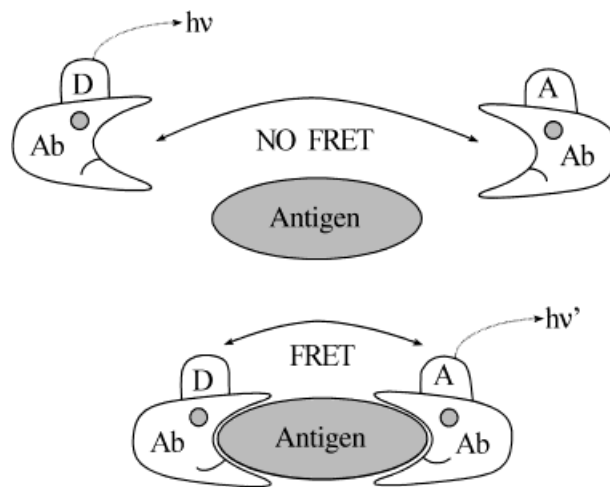


FIG. 8. FRET-based homogeneous immunoassay for polyhaptenic antigen. Two monoclonal antibodies raised against the antigen and labeled respectively with donor and acceptor fluorophore. FRET is observed only in the presence of the antigen.

better spectral overlap with the fluorescein emission spectra,  $R_0$  value of 6.2 nm was determined as compared to that of 5.4 nm for the fluorescein rhodamine pair. The higher  $R_0$  value made it possible to achieve efficient quenching of the fluorescent antigen without overlabeling the antibodies, increasing the stability and bench lifetime of the acceptor labeled antibody. The usefulness of this new probe was demonstrated in assaying morphine (55).

The other approach to improve FRET-based immunoassay took advantage of excellent spectral properties of phycobilliprotein fluorescent dyes (57). Two dye combinations were used to demonstrate the basic principles involved. In the first, fluorescein-conjugated human immunoglobulin G (IgG) was quenched by a conjugate of PE and

goat anti-human IgG. In the second, the fluorescence of PE conjugate to human IgG was quenched by Texas Red-labeled goat anti-human IgG. The reason PE can be used as either donor or acceptor is that the absorption spectrum of PE overlaps the emission spectrum of fluorescein and the absorption spectrum of Texas Red overlaps the emission spectrum of PE. Both approaches produced sensitive and reliable assays for human IgG. In the latter combination, a potential advantage of the system is operation in the red end of this spectrum, where biological interferences should be much less. This is most important in homogeneous assays in which the assay mixture is not separated from the tested serum. In addition, the phycobiliproteins give more intense signals and less nonspecific binding. Immunity from random collision quenching with ions of the serum should also be significantly decreased because chromophores in phycobiliproteins are protected by the proteins to which they are attached (57).

FRET immunoassays based upon acceptor fluorescence emission are plagued with background fluorescence resulting from absorption of the excitation light by the acceptor dye. To overcome this problem a long-lifetime donor fluorophore (pyrenebutyrate) and a short-lifetime acceptor fluorophore (PE) were applied in combination with pulsed-laser excitation and electronic gating of detector signals. This permitted the separation of the component of acceptor emission due to energy transfer from the component arising from the absorption of the excitation light (75). Human IgG was measured in a competitive assay using pyrene-conjugated F(ab')<sub>2</sub> fragments against human IgG and PE-conjugated human IgG as a tracer. Acceptor emission was measured with 0- and 20-ns integration delays and the ratios of the FRET components to the laser-excited component increased by 9- to 15-fold when the 20-ns delay was used in the immunoassay and the sensitivity was in the order of 10 nM. Increasing, the sensitivity required lowering the concentration of labeled antigen and antibody reagents. Although the fluorometer can detect the acceptor fluorescence at a concentration thousand-fold lower than those used by the assay described above, the formation of appreciable amounts of antibody-antigen complexes at lower reagent concentrations required the use of antibodies with affinity constants considerably higher than those applied by Morrison (75).

Energy transfer process between PE-conjugated thyroxine and Cy5-conjugated anti-thyroxine antibody was used to measure thyroxine concentration using competitive assay format (81). In this assay format, however, the fluorescence intensity change was not monitored but the fluorescence lifetime was determined by multifrequency phase-modulation fluorescence. Dose-response curves of phase angle versus thyroxine concentration were comparable to steady-state fluorescence intensity curves. Because phase modulation lifetime measurements are largely independent of total signal intensity, sources of optical interference are minimized (81). This approach was further improved when long-lifetime luminescent metal-ligand complexes were used in a FRET-based immunoassay for human serum albumin (128). Human serum albumin

(HSA) was labeled with [Ru(bpy)<sub>2</sub>(phen-ITC)]<sup>2+</sup>, and the antibody to HSA with a nonfluorescent absorber, Reactive Blue 4. The concentration of HSA was determined in a competitive assay in which the presence of analyte prevented the decrease of fluorescence lifetime by immune complex formation. The advantages of the ruthenium-ligand fluorophore include its long wavelength absorption and emission, long fluorescence lifetime, and high photostability. Long wavelengths minimize problems of autofluorescence from biological samples, and long lifetimes allow off-gating of the prompt autofluorescence (128).

Mathis also used rare earth (Eu) cryptates to develop FRET immunoassay allowing double discrimination of the emitted light through spectral and temporal selectivity (67,68). Eu(III) trisbipyridine cryptate [TBP(Eu(III))]-conjugated antibody was used as donor, and APC-labeled antibody was used as acceptor. Both antibodies bind prolactin and in the presence of prolactin an immune complex is formed and energy transfer can take place. Because sensitized emission of APC is detected, the method is called as amplified homogeneous assay. Time-resolved detection eliminates the direct fluorescence of unbound APC-antibody, spectral selection eliminates the luminescence of TBP(Eu(III)). The author introduced double wavelength detection, which fully shields the assay from perturbations of the media. This feature of the assay is based on the following phenomenon: because of the amount of the analyte and the bound donor-labeled antibody is always small compared to the overall concentration of the donor-labeled antibody, the free donor-labeled antibody concentration can be taken as a constant. The emission yield of free donor becomes an internal luminescence standard that takes into account quenching artifacts due to absorptions by interfering species in the sample to be analyzed. These features have allowed the development of a rapid homogeneous immunoassay that can detect as little as 0.3 µg/l of prolactin. A plate reader has also been developed to permit simultaneous dual-wavelength time-resolved luminescence detection for this assay (25,67,68).

In FRET immunoassays, random labeling of whole antibody with a fluorescent donor could result in some donor moieties that are so distant from the binding site that they are unable of undergoing energy transfer to bound acceptor-conjugated antigen. This circumstance is unsatisfactory because there would be no change in intensity and lifetime for that donor population. Thus the extent of immune complex formation would be poorly determined and the dynamic range of the assay would be reduced. In contrast, site-specific labeling results in greater homogeneity of FRET distances. To achieve this goal, Chang and coworkers applied photoaffinity labeling in which fluorescein was conjugated to the biotin hapten and tetramethylrhodamine was attached to anti-biotin antibodies (13). An energy transfer efficiency of almost 50% was observed upon binding of fluoresceinated biotin, which indicated that the photoaffinity labeling technique attached tetramethylrhodamine groups at positions within energy transfer distance (5.2 nm) from the antigen-combining site.

A novel concept was described for directly coupling fluorescence enhancement to protein-ligand binding (121). Wei and coworkers used the phenomenon that some fluorescent dyes (e.g., fluorescein and rhodamine molecules) form dimers in aqueous solution when they are at high concentrations or within close proximity to each other, resulting in significant quenching of the fluorophores. This sometimes adverse effect can be used to advantage to quench the fluorescence of free tracers and to enhance the fluorescence of bound tracers if the dimer  $\rightleftharpoons$  monomer equilibrium can be modulated by antibody antigen reactions. Toward this end, a 13-residue peptide, recognized by a monoclonal antibody against human chorionic gonadotrophin (hCG) was labeled with fluorescein and tetramethylrhodamine at its N- and C-termini. Due to intramolecular dimerization, the fluorescence of fluorescein and rhodamine was quenched by 98% and 90%, respectively. Binding of anti-hCG antibody to the labeled peptide resulted in a 7.8-fold increase in rhodamine fluorescence due to dissociation of intramolecular dimers brought about conformational changes of the conjugate upon binding. Fluorescein fluorescence was still quenched because of the FRET to rhodamine. In the assay mixture the presence of the analyte (hCG) will inhibit the enhancement in rhodamine fluorescence. The double-labeled peptide technique is a promising assay, especially of large molecular analytes, given that fluorescence homogeneous assays are simple, reproducible, and can readily be adapted to 96-well fluorescence plate readers (121).

**DNA analysis.** DNA analysis is becoming increasingly important in the diagnosis of hereditary diseases, detection of infections agents, tissue typing for histocompatibility, identification of individuals in forensic and paternity testing, and monitoring the genetic composition of plants and animals in agricultural breeding programs. DNA analysis usually involves DNA sequencing, polymerase chain reaction (PCR), and DNA hybridization or combinations of these techniques. Application of FRET-based fluorescent probes fertilized and revolutionized all of these fields: the fluorescence-based DNA sequencing, quantitative monitoring of PCR reactions, and the assay of DNA denaturation. For flow cytometry, until recently much of the nucleic acid-based technology was available only for research applications such as the PCR-driven fluorescent in situ hybridization (FISH) method (76). With color-coded bead technology, it is possible to prepare DNA hybridization and ligand binding interactions. The principle is the same as that utilized by immunoassays. The ligand-ligate interaction occurs not between an antigen and an antibody but between oligonucleotides in a hybridization situation.

The human genome project is driving the development of high-speed and high-output DNA sequencing and analysis methods. Currently, the Sanger dideoxy chain-termination method is accepted as the technique of choice for all large-scale sequencing projects (87,88). The dideoxy sequencing involves the use of 2',3'-dideoxynucleoside triphosphates (ddNTPs), which lack a 3'-hydroxyl group. In this method, the single-stranded DNA to be sequenced serves as the template strand or in vitro DNA synthesis: a

synthetic 5'-end-labeled oligodeoxynucleotide is used as the primer. Four separate polymerization reactions are performed, each with a low concentration of one of the four ddNTPs in addition to higher concentrations of the normal deoxynucleoside triphosphates (dNTPs). In each reaction the ddNTP is randomly incorporated at the positions of the corresponding dNTP; such addition of ddNTP terminates polymerization because the absence of 3' hydroxyl prevents addition of the next nucleotide. The newly synthesized DNA can be fluorescently labeled with any of four differently end-labeled fluorescent primers (91) or terminators (85). The mixture of terminated fragments from each of the four reactions is subjected to gel or capillary electrophoresis in parallel; the separated fragments then are detected using appropriate excitation (usually laser) and detection systems. The sequence of the original DNA template strand can directly be read from the resulting chromatogram. The detection sensitivity is limited by the spectroscopic properties of the available fluorescent dyes for labeling the sequencing fragments. Ideally each of the four dyes should exhibit strong absorption at a common laser wavelength, have an emission maximum at a distinctly different wavelength, and introduce the same relative electrophoretic mobility shift of the DNA sequencing fragments. Because these criteria are inconsistent with the spectroscopic properties of single fluorescent dye molecules, Ju and coworkers have designed and synthesized FRET-based primers for application to four-color DNA sequencing (51). These primers carry a fluorescein derivative (FAM [5-carboxyfluorescein]) at the 5' end as a common donor and other fluorescein (JOE [2',7'-dimethoxy-4',5'-dichloro-6-carboxyfluorescein]) and rhodamine (TAMRA [*N,N,N',N'*-tetramethyl-6-carboxyrhodamine] or ROX [6-carboxy-X-rhodamine]) derivatives attached to a modified thymidine residue within the primer sequence as acceptors. By adjusting the donor-acceptor spacing through the placement of the modified thymidine in the primer sequence the authors were able to generate four primers, all having strong absorption at a common excitation (488 nm), similar electrophoretic mobility, and fluorescence emission maxima at 525, 555, 580, and 605 nm. The FRET efficiency of these primers ranges from 65% to 97%. The fluorescence intensity of these FRET primers is 2- to 6-fold greater than that of the corresponding primers or fragments labeled with single dyes allowing DNA sequencing with one-fourth of DNA template required (51,52). This approach has successfully been combined with capillary electrophoresis chips for ultra-high-speed DNA sequencing (125) and applied for rapid sizing of short tandem repeat alleles (118-120). The same group of investigators modified their method for FRET primer synthesis by constructing fluorescent primers using a universal ET cassette that can be incorporated by conventional synthesis at the 5'-end of an oligonucleotide primer of any sequence. In this cassette, the donor and acceptor fluorophores are separated by a polymer spacer ( $S_0$ ) formed by six 1',2'-dideoxyribose phosphate monomers (50). The resulting primers using FAM as a donor and FAM, JOE, TAMRA or ROX as acceptors display well-separated

acceptor emission spectra with 2- to 12-fold enhanced fluorescence intensity relative to that of the corresponding single dye-labeled primers (49,50). To improve match in electrophoretic mobility of extended DNA fragments with those of the DNA sequencing fragments extended from other ET primers, the acceptor JOE was replaced by 5- and 6-carboxyrhodamine-6G (R6G). With single-stranded M13mp18 DNA as the template, a typical run with the new FRET primer with the other FRET primers on a capillary sequencer provided DNA sequences with 99% accuracy in the first 620 bases (43). The next improvement in FRET primers was the introduction of cyanine dyes with large absorption cross-sections as donor chromophores. The new ET primers have 3-( $\epsilon$ -carboxypentyl)-3'-ethyl-5',5'-dimethylloxycarbocyanine (CYA) at the 5'-end as a common energy donor and FAM, R6G, TAMRA, and ROX dyes as acceptors. With 488-nm excitation, the fluorescence intensity of these four FRET primers is 1.4- to 24-fold stronger than that of the corresponding primers only with single acceptor dye (44,45). The CYA-ROX primers offer better combination of acceptor fluorescence emission intensity and spectral purity than primers using BODIPY analogs as energy transfer pairs (43). The improvement of the spectroscopic properties of fluorescent tags provided by FRET primers has led to a quantum advance in the detection capabilities in DNA sequencing. These FRET primers are generally applicable to all analyses that employ fluorescent primers and should increase the sensitivity and throughput (50).

Polymerase chain reaction has gained wide acceptance as an exponential nucleic acid amplification technique and is used very frequently for research and clinical applications. Although PCR is mainly used as a qualitative tool, there is a need for obtaining semiquantitative or even quantitative information. To eliminate the application of radioactive primers or radioactive nucleotides, detection systems based on fluorescence have been elaborated for quantitation the products of PCR reaction. Chan and coworkers 5'-end-labeled a PCR primer with the europium chelator 4,7-bis(chlorosulphophenyl)-1,10-phenanthroline-2,9-dicarboxylic acid (BCPDA) (12). After performing the PCR and separating the PCR products with gel electrophoresis the gel was immersed into a  $\text{Eu}^{3+}$  solution. During soaking the  $\text{Eu}^{3+}$  diffused into the gel formed a fluorescent complex of long fluorescence lifetime with BCPDA. This complex was quantified by scanning the gel with a time-resolved fluorometric reader. Because the BCPDA and  $\text{Eu}^{3+}$  are not fluorescent themselves, the background signal was very low, and the detection limit was about 5 ng of DNA (12). The europium in combination with an other chelator (with trisbipyridine cryptate) has successfully been applied in PCR reaction for the detection of human papillomavirus type 16 DNA in clinical smears. In this approach, nested PCR was performed with use of biotinylated and 2,4-dinitrophenol (DNP)-labeled oligonucleotides and then the biotinylated strands were anchored to avidin-coated microtiter plates. DNA hybrids containing both the biotinylated strand and the DNP-labeled strand were labeled with TBP( $\text{Eu}^{3+}$ )-labeled anti-DNP antibody.

PCR product was quantified by measuring fluorescence according to the principle of time-resolved fluorometry (65). In the above instances only the end products of the PCR reaction were measured, although there is a demand for continuous monitoring the DNA amplification process. Toward this end, Wittwer and coworkers have developed three fluorescent approaches for monitoring rapid cycle DNA amplification (122). The reaction was followed by either measuring the fluorescence of SYBR Green dye incorporating into double-stranded DNA; monitoring the decrease in fluorescein quenching by rhodamine after exonuclease cleavage of a dual-labeled hydrolysis probe; or quantitating the resonance energy transfer between fluorescein and Cy5 dyes by adjacent hybridization probes. The specificity of the last two methods using the FRET principle was much better than that of the first method. With hydrolysis probes, fluorescence continues to increase after the plateau phase is reached, whereas with hybridization probes, fluorescence decreases during the plateau phase. Despite these limitations, initial template copy number can be quantified easily by measuring fluorescence at each amplification cycle (122). Based on this principle Wittwer and coworkers developed a commercial microvolume fluorimeter (LightCycler<sup>TM</sup>) with rapid temperature control interrogating 1 to 10  $\mu\text{l}$  samples in glass capillaries (123). In this instrument a complete amplification and analysis requires only 10 to 15 min (123).

Detection of point mutation and deletion or insertion of basepairs in specific DNA fragments can accurately be achieved via DNA sequencing. If only the presence or the absence of such alterations is to be detected, monitoring DNA denaturation could be the right solution. Hiyoshi and Hosoi used fluorescein-11-dUTP and rhodamine-4-dUTP to label complementary DNA strands using PCR (42). The complementary strands thus labeled were then annealed by incubation at a constant temperature, and the energy transfer efficiency was monitored during DNA denaturation induced by heat or alkali treatments. The method proved to be a simple and efficient procedure for monitoring DNA denaturation for use in automated detection and diagnosis systems (42).

Chen and Kwok have developed a novel detection strategy that allows the rapid analysis of single nucleotide polymorphisms in a homogeneous assay, eliminating the need for product separation and the use of radioactivity (15). Their approach combines the specificity of enzymatic discrimination between the two alleles of a single nucleotide polymorphism in a template-directed primer extension reaction and the sensitivity of fluorescence resonance energy transfer. DNA fragments containing polymorphic sites are incubated with a 5'-fluorescein-labeled primer (designed to hybridize to DNA template adjacent to the polymorphic site) in the presence of allelic dye (ROX)-labeled dideoxyribonucleoside triphosphates. The dye-labeled primer is extended one base by the dye-terminator specific for the allele present on the template. FRET occurs when the dye-labeled ddNTP is incorporated into the sequencing primer in the presence

of DNA polymerase and target DNA. Fluorescence intensity of the two dyes in the reaction mixture is analyzed directly without separation or purification. This template-directed dye-terminator incorporation assay is highly sensitive and specific and suitable for automated genotyping of large numbers of samples (15). The method has successfully been applied to detect mutations in the cystic fibrosis transmembrane conductance regulator gene (14).

DNA tests will no doubt be performed more and more by clinical rather than research laboratories, utilizing the multiplexed assays that require minimal laboratory skills, and manual handling will be crucial to the practice of medicine in the future.

#### NEW DEVELOPMENTS

Successful application of FRET is highly promoted by introduction of modern instrumentation in fluorescence detection systems. The advantage of fluorescence lifetime imaging (FLIM) over conventional steady-state fluorescence microscopy results from the fact that fluorescence lifetimes are usually independent of the fluorophore concentration, photobleaching, and other artifacts that affect fluorescence intensity measurements (89). Time-resolved fluorescence microscopy enables mapping of fluorescence lifetimes, which is vital for the determination of the spatial distribution of probe molecules. In addition, it can also be used to enhance contrast between fluorescence arising from distributions of different probe species having similar spectral characteristics and provides a means of discriminating against background autofluorescence. Because measuring changes in the fluorescence lifetime can monitor FRET efficiency, combination of FLIM with FRET measurements will open new fields for this type of approach. Whereas the first FLIM instruments were relatively slow, the latest developments in this field greatly enhanced the resolution time-domain FLIM measurement (89).

Application of near-field scanning optical microscopy (NSOM) extends the sensitivity of FRET to the single molecule level by measuring FRET between single donor and single acceptor molecules. NSOM is a relatively new technique that allows optical measurements with sub-wavelength resolution (37). It is based on a probe having very small (sub-wavelength) aperture that is placed in close proximity (less than 10 nm) to the sample under investigation. By using the probe as an excitation source, fluorescence of single molecules can be detected. Another important aspect of NSOM is that the optical radiation in the near field has an electric field component along its directions of propagation. This allows mapping the transition dipole moment orientation of a single molecule in three dimensions. Combination of FRET and NSOM offers many potential advantages when distance and orientation information is required on a molecular level (37).

It has been shown that photobleaching FRET measurements can be used to monitor intercellular proximity in order to assess spatial organization of interacting proteins in the contact region of two "communicating" cells (2). Interactions between CD8 and MHC class I molecules and also between LFA-1 and ICAM-1 molecules has successfully

been studied using fluoresceinated and rhodaminated mAbs. The geometry of these protein contacts based on FRET data was consistent with the observed blocking effects of monoclonal antibodies (directed against the interacting proteins) on the cytolytic activity of CTLs (2). Further development in this technique will be the introduction of confocal microscopy in studying intercellular interactions.

A new development in the field of photobleaching energy transfer measurements is the introduction of acceptor photobleaching (4). In this approach the increase in the fluorescence intensity of donor is measured following the local photochemical destruction of the energy acceptor. Donor fluorophores engaged in FRET exhibit an increase in quantum yield after acceptor photo-destruction, reflect as an increase of fluorescence. Photodestruction of the acceptor molecules can be performed in a region of interest (i.e., at any part of a cell). FRET efficiency can be calculated by taking the ratio of donor images before and after photobleaching without external calibration. In practice, experiments can be performed with a confocal microscope equipped with a multiple laser system providing lines corresponding to the absorption maxima of both donor and acceptor. The technique permits the exploitation FRET in the study of the processing and interactions of biomolecules in cells (4).

#### CONCLUSIONS

Since the first description of the phenomenon, the number of applications of FRET has been increased enormously in diverse research fields in the last few decades. A unique feature of FRET is its capability to detect, quantitatively, molecular interactions, over distances of tens of angstroms. Improving the sensitivity of the detection systems in spectrofluorometers, flow cytometers, and microscopes widen the field in which FRET can be applied. Improvements in FRET analysis, especially in temporal resolution of fluorescence data have increased considerably the possibilities for FRET measurements. In addition, introduction of new fluorescent dyes with better photophysical properties also promotes the application of FRET. Developments in microscopic techniques in the performance and availability of sophisticated image data acquisition and image analysis have also made it possible to contemplate more quantitative FRET experiments in optical microscopes. Introduction of confocal detection arrangement will also reinforce the FRET approach. These improvements in microscopic techniques open up new areas in biological problems that otherwise could not be investigated with the classical FRET method. Spatially resolved FRET measurements in an image provide important information about the distribution of molecular-scale interactions over distances of microns, helping in understanding the intricate interactions in functioning biological systems. For example, cell-cell interactions can be studied in a very special way using microscopic FRET technique, because the protein-protein interactions in the area of cell-cell contact can be investigated selectively.

These improvements and inventions will continue to facilitate the innovative applications of FRET in clinical laboratory and basic research.

#### ACKNOWLEDGMENTS

We thank Francis Mandy for critical reading of the manuscript and for his valuable suggestions.

#### LITERATURE CITED

- Armand S, Drouillard S, Schulein M, Henrissat B, Driguez H: A bifunctionalized fluorogenic tetrasaccharide as a substrate to study cellulases. *J Biol Chem* 272:2709–2713, 1997.
- Bacsó Z, Bene L, Bodnár A, Matkó J, Damjanovich S: A photobleaching energy transfer analysis of CD8/MHC-I and LFA-1/ICAM-1 interactions in CTL-target cell conjugates. *Immunol Lett* 54:151–156, 1996.
- Bacsó Z, Matkó J, Szöllösi J, Gáspár R, Damjanovich S: Changes in membrane potential of target cells promotes cytotoxic activity of effector T lymphocytes. *Immunol Lett* 51:175–180, 1996.
- Bastiaens PIH, Majouli IV, Verveer PJ, Söling H-D, Jovin TM: Imaging the intracellular trafficking and state of the AB<sub>5</sub> quaternary structure of cholera toxin. *EMBO J* 15:4246–4253, 1996.
- Beavis AJ, Pennline KJ: ALLO-7: A new fluorescent tandem dye for use in flow cytometry. *Cytometry* 24:390–394, 1996.
- Bene L, Balázs M, Matkó J, Möst J, Dierich M, Szöllösi J, Damjanovich S: Lateral organization of the ICAM-1 molecule at the surface of human lymphoblasts: A possible model for its co-distribution with the IL-2 receptor, class I and class II HLA molecules. *Eur J Immunol* 24:2115–2123, 1994.
- Bene L, Szöllösi J, Balázs M, Mátyus L, Gáspár R, Ameloot M, Dale RE, Damjanovich S: Major histocompatibility complex class I protein conformation altered by transmembrane potential changes. *Cytometry* 27:353–357, 1997.
- Bickett DM, Green MD, Wagner C, Roth JT, Berman J, McGeehan GM: A high throughput fluorogenic substrate for stromelysin (MMP-3). *Ann NY Acad Sci* 732:351–355, 1994.
- Bodnár A, Jenei A, Bene L, Damjanovich S, Matkó J: Modification of membrane cholesterol level affects expression and clustering of class I HLA molecules at the surface of JY human lymphoblasts. *Immunol Lett* 54:221–226, 1996.
- Bouvier J, Schneider P, Malcolm B: A fluorescent peptide substrate for the surface metalloproteinase of *Leishmania*. *Exp Parasitol* 76:146–155, 1993.
- Catipovic B, Talluri G, Oh J, Wei T, Su X-M, Johansen TE, Edidin M, Schneck JP: Analysis of the structure of empty and peptide-loaded Major Histocompatibility Complex molecules at the cell surface. *J Exp Med* 180:1753–1761, 1994.
- Chan A, Diamandis EP, Krajden M: Quantification of polymerase chain reaction products in agarose gels with a fluorescent europium chelate as label and time-resolved fluorescence spectroscopy. *Anal Chem* 65:158–163, 1993.
- Chang I-N, Lin J-N, Andrade JD, Herron JN: Photoaffinity labeling of antibodies for applications in homogeneous fluoroimmunoassays. *Anal Chem* 67:959–966, 1995.
- Chen X, Zehnbauser B, Gnirke A, Kwok P-Y: Fluorescence energy detection as a homogeneous DNA diagnostic method. *Proc Natl Acad Sci USA* 94:10756–10761, 1997.
- Chen X, Kwok P-Y: Template-directed dye-terminator incorporation (TDI) assay: A homogeneous DNA diagnostic method based on fluorescence resonance energy transfer. *Nucleic Acid Res* 25:347–353, 1997.
- Clark ID, Macmanus JP, Szabo AG: A protease assay using time-resolved lanthanide luminescence from an engineered calcium binding protein substrate. *Clin Biochem* 28:131–135, 1995.
- Clegg RM: Fluorescence energy transfer. *Curr Opin Biotech* 6:103–110, 1995.
- Clegg RM: Fluorescence Resonance Energy Transfer (FRET). In: *Fluorescence Spectroscopy and Microscopy*. Wang XF, Hermann B (eds). J. Wiley and Sons, New York, 1996. Chemical Analysis Series. Vol. 137:179–252.
- Dale RE, Eisinger J, Blumberg WE: The orientational freedom of molecular probes. The orientation factor in intramolecular energy transfer. *Biophys J* 26:161–194, 1979.
- Dale RE, Novros J, Roth S, Edidin M, Brand L: Application of Förster Long-Range Excitation Energy Transfer to the Determination of Distributions of Fluorescently-Labeled Concanavalin A-Receptor Complexes at the Surfaces of Yeast and of Normal and Malignant Fibroblasts. In: *Fluorescent Probes*, Beddard GS, West A (eds). Academic Press, London, 1981, pp 159–189.
- Damjanovich S, Gáspár R, Pieri C: Dynamic receptor superstructure at plasma membrane. *Q Rev Biophys* 30:67–106, 1997.
- Damjanovich S, Trón L, Szöllösi J, Zidovetzki R, Vaz WLC, Regateiro F, Arndt-Jovin DJ, Jovin TM: Distribution and mobility of murine histocompatibility H-2K<sup>b</sup> antigen in the cytoplasmic membrane. *Proc Natl Acad Sci USA* 80:5985–5989, 1983.
- Damjanovich S, Vereb G, Shaper A, Jenei A, Matkó J, Starink JPP, Fox GO, Arndt-Jovin DJ, Jovin TM: Structural hierarchy in the clustering of HLA class I molecules in the plasma membrane of human lymphoblastoid cells. *Proc Natl Acad Sci USA* 92:1122–1126, 1995.
- Dewey TG, Hammes GG: Calculation of fluorescence resonance energy transfer on surfaces. *Biophys J* 32:1023–1035, 1980.
- Dickson EFG, Pollak A, Diamandis P: Time-resolved detection of lanthanide luminescence for ultrasensitive bioanalytical assays. *J Photochem Photobiol B: Biol* 27:3–19, 1995.
- Doody MC, Sklar LA, Pownall HJ, Sparrow JT, Gotto AM Jr, Smith LC: A simplified approach to resonance energy transfer in membranes, lipoproteins and spatially restricted systems. *Biophys Chem* 17:139–152, 1983.
- Estep TN, Thompson TE: Energy transfer in lipid bilayers. *Biophys J* 26:195–208, 1979.
- Fairclough RH, Cantor CR: The use of singlet-singlet energy transfer to study macromolecular assemblies. *Methods Enzymol* 48:347–379, 1978.
- Förster T: Energiewanderung und Fluoreszenz. *Naturwissenschaften* 6:166–175, 1946.
- Förster T: Zwischenmolekulare Energiewanderung und Fluoreszenz. *Ann Phys (Leipzig)* 2:55–75, 1948.
- Fulton RJ, McDade RL, Smith PL, Kienker LJ, Kettman JR: Advanced multiplexed analysis with the FlowMatrix system. *Clin Chem* 43:1749–1756, 1997.
- Ghosh SS, Eis PS, Blumeyer K, Fearon K, Millar DP: Real time kinetics of restriction endonuclease cleavage monitored by fluorescence resonance energy transfer. *Nucleic Acid Res* 22:3155–3159, 1994.
- Goudreau N, Guis C, Soleilhac J-M, Roques BP: Dns-Gly-(p-NO<sub>2</sub>)Phe-βAla, a specific fluorogenic substrate for neutral endopeptidase 24.11. *Anal Biochem* 219:87–95, 1994.
- Guo C, Dower SK, Holowka D, Baird B: Fluorescence resonance energy transfer reveals interleukin (IL)-1-dependent aggregation of IL-1 type I receptors that correlates with receptor activation. *J Biol Chem* 270:27562–27568, 1995.
- Gutierrez-Merino C: Quantitation of the Förster energy transfer for two dimensional systems. I. Lateral phase separation in unilamellar vesicles formed by binary phospholipid mixtures. *Biophys Chem* 14:247–257, 1981.
- Gutierrez-Merino C: Quantitation of the Förster energy transfer for two dimensional systems. II. Protein distribution and aggregation state in biological membranes. *Biophys Chem* 14:259–266, 1981.
- Ha T, Enderle DF, Opletree DF, Chemla DS, Selvin PR, Weiss S: Probing the interaction between two single molecules: fluorescence resonance energy transfer between a single donor and a single acceptor. *Proc Natl Acad Sci USA* 93:6264–6268, 1996.
- Haver VM, Audino N, Burris S, Nelson M: Four fluorescence polarization immunoassays for therapeutic drug monitoring evaluated. *Clin Chem* 35:138–140, 1989.
- Hemmilä I: Fluoroimmunoassay and immunofluorometric assays. *Clin Chem* 31:359–370, 1985.
- Hemmilä I, Malmgren O, Mikola H, Lövgren T: Homogeneous time-resolved fluoroimmunoassay of thyroxine in serum. *Clin Chem* 34:2320–2322, 1988.
- Hirschfeld T: Quantum efficiency independence of the time integrated emission from a fluorescent molecule. *Applied Optics* 15:3135–3139, 1976.
- Hiyoshi M, Hosoi S: Assay of DNA denaturation by polymerase chain reaction-driven fluorescent label incorporation and fluorescence resonance energy transfer. *Anal Biochem* 221:306–311, 1994.
- Hung S-C, Ju J, Mathies RA, Glazer AN: Energy transfer primers with 5- or 6- carboxyrhodamine-6G as acceptor chromophores. *Anal Biochem* 238:165–170, 1996.
- Hung S-C, Ju J, Mathies RA, Glazer AN: Cyanine dyes with high absorption cross section as donor chromophores in energy transfer primers. *Anal Biochem* 243:15–17, 1996.
- Hung S-C, Mathies RA, Glazer AN: Comparison of fluorescence energy transfer primers with different donor-acceptor dye combinations. *Anal Biochem* 255:32–38, 1998.
- Jenei A, Varga S, Bene L, Mátyus L, Bodnár A, Bacsó Z, Pieri C, Gáspár R, Farkas T, Damjanovich S: HLA class I and II antigens are partially co-clustered in the plasma membrane of human lymphoblastoid cells. *Proc Natl Acad Sci USA* 94:7269–7274, 1997.
- Jovin TM, Arndt-Jovin DJ: Luminescence digital imaging microscopy. *Ann Rev Biophys Chem* 18:271–308, 1989.

48. Jovin TM, Arndt-Jovin DJ: FRET microscopy: Digital imaging of fluorescence resonance energy transfer. Application in cell biology. In: Kohen E, Ploem JS and Hirschberg JG (eds.), *Microspectrofluorometry of single living cells*, Academic Press, Orlando, 1989, pp. 99–117.
49. Ju J, Glazer AN, Mathies RA: Cassette labeling for facile construction of energy transfer fluorescent primers. *Nucleic Acid Res* 24:1144–1148, 1996.
50. Ju J, Glazer AN, Mathies RA: Energy transfer primers: A new fluorescence labeling paradigm for DNA sequencing and analysis. *Nature Med* 2:246–249, 1996.
51. Ju J, Kheterpal I, Scherer JR, Ruan C, Fuller CW, Glazer AN, Mathies RA: Design and synthesis of fluorescence energy transfer dye-labeled primers and their application for DNA sequencing and analysis. *Anal Biochem* 231:131–140, 1995.
52. Ju J, Ruan C, Fuller CW, Glazer AN, Mathies RA: Fluorescence energy transfer dye-labeled primers for DNA sequencing and analysis. *Proc Natl Acad Sci USA* 92:4347–4351, 1995.
53. Jürgens L, Arndt-Jovin D, Pecht I, Jovin TM: Proximity between the type I receptor  $Fc_\epsilon$  ( $Fc_\epsilon R$ ) and the mast cell function-associated antigen (MAFA) studied by donor photobleaching fluorescence resonance energy transfer microscopy. *Eur J Immunol* 26:84–91, 1996.
54. Kam Z, Volberg T, Geiger B: Mapping of adherent junction components using microscopic resonance energy transfer imaging. *J Cell Sci* 108:1051–1062, 1995.
55. Khanna PL, Ullman EF: 4',5'-Dimethoxy-6-carboxyfluorescein: A novel dipole-dipole coupled fluorescence energy transfer acceptor useful for fluorescence immunoassays. *Anal Biochem* 108:156–161, 1980.
56. Kindzelskii AL, Laska ZO, Todd RF, Petty HR: Urokinase-type plasminogen activator receptor reversibly dissociates from complement receptor type 3 ( $\alpha_M\beta_2$ ; CD11b/CD18) during neutrophil polarization. *J Immunol* 156:297–309, 1996.
57. Kronick MN, Grossman PD: Immunoassay techniques with fluorescent phycobiliprotein conjugates. *Clin Chem* 29:1582–1586, 1983.
58. Lakowicz JR: *Principles of Fluorescence Spectroscopy*, Plenum Press, New York, 1983, pp. 303–339.
59. Lazarovits AI, Osman N, Le Feuvre CE, Ley SC, Crumpton MJ: CD7 is associated with CD3 and CD45 on human T cells. *J Immunol* 153:3956–3964, 1994.
60. Lansdorp PM, Smith C, Safford M, Terstappen LW, Thomas TE: Single laser three immunofluorescence staining procedures based on energy transfer between phycoerythrin and cyanine-5. *Cytometry* 12:723–730, 1991.
61. Lee KB, Matsuoka K, Nishimura SI, Lee YC: A new approach to assay endo-type carbohydrases: bifluorescent-labeled substrates for glycoamidases and ceramide glycanases. *Anal Biochem* 230:31–36, 1995.
62. Lee SP, Censullo ML, Kim HG, Knutson JR, Han MK: Characterization of endonucleolytic activity of HIV-1 integrase using a fluorogenic substrate. *Anal Biochem* 227:295–301, 1995.
63. Liburdy RP: Antibody induced fluorescence enhancement of a N-(3-pyrene) maleimide conjugate of rabbit anti-human immunoglobulin G: Quantitations of human IgG. *J Immunol Methods* 28:233–242, 1979.
64. Lim CS, Miller JN, Bridges JW: Energy-transfer immunoassay: A study of the experimental parameters in an assay for human serum albumin. *Anal Biochem* 108:176–184, 1980.
65. Lopez E, Chypre C, Alpha B, Mathis G: Europium(III) trisbipyridine cryptate label for time-resolved fluorescence detection of polymerase chain reaction products fixed on a solid support. *Clin Chem* 39:196–201, 1993.
66. Matayoshi ED, Wang GT, Krafft GA, Erickson J: Novel fluorogenic substrates for assaying retroviral proteases by resonance energy transfer. *Science* 247:954–958, 1990.
67. Mathis G: Rare earth cryptates and homogeneous fluorimmunoassays with human sera. *Clin Chem* 39:1953–1959, 1993.
68. Mathis G: Probing molecular interactions with homogeneous techniques based on rare earth cryptates and fluorescence energy transfer. *Clin Chem* 41:1391–1397, 1995.
69. Matkó J, Edidin M: Energy transfer methods for detecting molecular clusters on cell surfaces. *Methods Enzymol* 278:444–462, 1997.
70. Matkó J, Szöllösi J, Trón L, Damjanovich S: Luminescence spectroscopic approaches of cell surface molecules. *Quart Rev Biophys* 21:479–544, 1988.
71. Mátyus L: Fluorescence resonance energy transfer measurements on cell surfaces. A spectroscopic tool for determining protein interactions. *J Photochem Photobiol B: Biol* 19:67–73, 1992.
72. Mátyus L, Bene L, Heiligen H, Rausch J, Damjanovich S: Distinct association of transferrin receptor with HLA class I molecules on HUT-102B and JY cells. *Immunol Lett* 44:203–208, 1995.
73. McDade RL, Fulton RJ: True multiplexed analysis by computer-enhanced flow cytometry. *Med Dev Diag Indust* 19:75–82, 1997.
74. Mitra RD, Silva CM, Youvan DC: Fluorescence resonance energy transfer between blue-emitting and red-shifted excitation derivatives of the green fluorescent protein. *Gene* 173:13–17, 1996.
75. Morrison LE: Time-resolved detection of energy transfer: Theory and application to immunoassays. *Anal Biochem* 174:101–120, 1988.
76. Mosiman VL, Patterson BK, Canterero L, Goolsby C: Reducing cellular autofluorescence in flow cytometry: An *in situ* method. *Cytometry* 30:151–156, 1997.
77. Neppert J, Müller-Eckhardt C: Monoclonal antibodies to human class I antigens cocap class II antigens. *Tissue Antigens* 24:187–189, 1984.
78. Neppert J, Müller-Eckhardt C: Interdependent membrane mobility of human MHC coded antigens detected by monoclonal antibodies to various epitopes on class I and class II molecules. *Tissue Antigens* 26:51–69, 1985.
79. Niles DW, Silvius JR, Cohen FS: Resonance energy transfer imaging of phospholipid vesicle interaction with a planar phospholipid membrane. Undulations and attachment sites in the region of calcium-mediated membrane-membrane adhesion. *J Gen Physiol* 107:329–351, 1996.
80. Oi VT, Glazer AN, Stryer L: Fluorescent phycobiliprotein conjugates for analyses of cells and molecules. *J Cell Biol* 93:981–986, 1982.
81. Ozinskas AJ, Malak H, Joshi J, Szmacinski H, Britz J, Thompson RB, Koen PA, Lakowicz JR: Homogeneous model immunoassay of thyroxine by phase modulation fluorescence spectroscopy. *Anal Biochem* 213:264–270, 1983.
82. Pennington MW, Thornberry NA: Synthesis of a fluorogenic interleukin-1 $\beta$  converting enzyme substrate based on resonance energy transfer. *Peptide Res* 7:72–76, 1994.
83. Poo H, Fox B, Petty HR: Ligation of CD3 triggers transmembrane proximity between LFA-1 and cortical microfilaments in a cytotoxic T cell clone derived from tumor infiltrating lymphocytes: A quantitative resonance energy transfer study. *J Cell Physiol* 159:176–180, 1994.
84. Poo H, Krauss JC, Mayo-Bond L, Todd RF, Petty HR: Interaction of  $Fc_\gamma$  receptor type IIB with complement receptor type 3 in fibroblast transfectants: Evidence from lateral diffusion and resonance energy transfer studies. *J Mol Biol* 247:597–603, 1995.
85. Prober JM, Trainor GL, Dam RJ, Hobbs FW, Robertson CW, Zagursky RJ, Cocuzza AJ, Jensen MA, Baumeister K: A system for rapid DNA sequencing with fluorescent chain-terminating dideoxynucleotides. *Science* 238:336–341, 1987.
86. Roederer M, Kantor AB, Parks DR, Herzenberg LA: Cy7PE and Cy7APC: Bright new probes for immunofluorescence. *Cytometry* 24:191–197, 1996.
87. Sanger F, Coulson AR: A rapid method for determining sequences in DNA by primed synthesis with DNA polymerase. *J Mol Biol* 94:441–448, 1975.
88. Sanger F, Nicklen S, Coulson AR: DNA sequencing with chain-terminating inhibitors. *Proc Natl Acad Sci USA* 74:5463–5467, 1977.
89. Scully AD, Ostler RB, Phillips D, O'Neill P, Townsend KMS, Parker AW, MacRobert AJ: Application of fluorescence lifetime imaging microscopy to the investigation of intracellular PDT mechanisms. *Bioimaging* 5:9–18, 1997.
90. Selvin PR: Fluorescence resonance energy transfer. *Methods Enzymol* 246:300–334, 1995.
91. Smith LM, Sanders JZ, Kaiser RJ, Hughes P, Dodd C, Connell CR, Heiner C, Kent SB, Hood LE: Fluorescence detection in automated DNA sequence analysis. *Nature* 321:674–679, 1986.
92. Snyder B, Freire E: Fluorescence energy transfer in two dimensions. A numeric solution for random and nonrandom distributions. *Biophys J* 40:137–148, 1982.
93. Stack MS, Gray RD: Comparison of vertebrate collagenase and gelatinase using a new fluorogenic substrate peptide. *J Biol Chem* 264:4277–4281, 1989.
94. Stryer L: Fluorescence energy transfer as a spectroscopic ruler. *Annu Rev Biochem* 47:819–846, 1978.
95. Szabó G, Pine PS, Weaver JL, Rao PE, Aszalos A: CD4 changes conformation upon ligand binding. *J Immunol* 149:3596–3604, 1992.
96. Szabó G, Pine PS, Weaver JL, Rao PE, Aszalos A: The L-selectin (Leu8) molecule is associated with the TCR/CD3 receptor: Fluorescence energy transfer measurements on live cells. *Immunol Cell Biol* 72:319–325, 1994.
97. Szabó G, Weaver JL, Pine PS, Rao PE, Aszalos A: Cross-linking of CD4 in a TCR/CD3-juxtaposed inhibitory state: A pFRET study. *Biophys J* 68:1170–1176, 1995.

98. Szöllösi J, Damjanovich S: Mapping of Membrane Structures by Energy Transfer Measurements. In: *Mobility and Proximity in Biological Membranes*, Damjanovich S, Szöllösi J, Trón L, Edidin M (eds). CRC Press, Boca Raton, 1994, pp. 49–108.
99. Szöllösi J, Damjanovich S, Balázs M, Nagy P, Trón L, Fulwyler MJ, Brodsky FM: Physical association between MHC class I and class II molecules detected on the cell surface by flow cytometry energy transfer. *J Immunol* 143:208–213, 1989.
100. Szöllösi J, Damjanovich S, Mulhern SA, Trón L: Fluorescence energy transfer and membrane potential measurements monitor dynamic properties of cell membranes: A critical review. *Prog Biophys Mol Biol* 49:65–87, 1987.
101. Szöllösi J, Horejsi V, Bene L, Angelisova P, Damjanovich S: Supramolecular complexes of MHC class I, MHC class II, CD20, and tetraspan molecules (CD53, CD81, and CD82) at the surface of a B cell line JY. *J Immunol* 157:2939–2946, 1996.
102. Szöllösi J, Mátyus L, Trón L, Balázs M, Ember I, Fulwyler MJ, Damjanovich S: Flow cytometric measurements of fluorescence energy transfer using single laser excitation. *Cytometry* 8:120–128, 1987.
103. Szöllösi J, Trón L, Damjanovich S, Helliwell SH, Arndt-Jovin DJ, Jovin TM: Fluorescence energy transfer measurements on cell surfaces. A critical comparison of steady-state and flow cytometric methods. *Cytometry* 5:210–216, 1984.
104. Taliani M, Bianchi E, Narjes F, Fossatelli M, Urbani A, Steinkuhler C, De Francesco R, Pessi A: A continuous assay of hepatitis C virus protease based on resonance energy transfer depsi-peptide substrates. *Anal Biochem* 240:60–67, 1996.
105. Tampé R, Clark BR, McConnell HM: Energy transfer between two peptides bound to one MHC class II molecule. *Science* 254:87–89, 1991.
106. Trón L: Experimental Methods to Measure Fluorescence Resonance Energy Transfer. In: *Mobility and Proximity in Biological Membranes*, Damjanovich S, Szöllösi J, Trón L, Edidin M (eds). CRC Press, Boca Raton, 1994, pp. 1–47.
107. Trón L, Aszalós A, Balázs M, Mulhern SA, Szöllösi J, Damjanovich S: On the biophysics of transmembrane signalling. *Mol Immunol* 25:1075–1080, 1988.
108. Trón L, Szöllösi J, Damjanovich S: Proximity measurements of cell surface proteins by fluorescence energy transfer. *Immunol Lett* 16:1–9, 1987.
109. Trón L, Szöllösi J, Damjanovich S, Helliwell SH, Arndt-Jovin DJ, Jovin TM: Flow cytometric measurement of fluorescence resonance energy transfer on cell surfaces. Quantitative evaluation of the transfer efficiency on a cell-by-cell basis. *Biophys J* 45:939–946, 1984.
110. Ullman EF, Khanna PL: Fluorescence excitation transfer immunoassay (FETI). *Methods Enzymol* 74:28–60, 1981.
111. Ullman EF, Schwarzbarg M, Rubenstein KE: Fluorescent excitation transfer immunoassay. A general method for determination of antigens. *J Biol Chem* 251:4172–4178, 1976.
112. Uster PS, Pagano RE: Resonance energy transfer microscopy: Observations of membrane-bound fluorescent probes in model membranes and in living cells. *J Cell Biol* 103:1221–1234, 1986.
113. Uster PS, Pagano RE: Resonance energy transfer microscopy: Visual colocalization of fluorescent lipid probes in liposomes. *Methods Enzymol* 171:850–857, 1989.
114. Vignali DAA, Carson RT, Chang B, Mittler RS, Strominger JL: The two membrane proximal domains of CD4 interact with the T cell receptor. *J Exp Med* 183:1097–2107, 1996.
115. Waggoner AS, Ernst LA, Chen LA, Rechtenwald DJ: PE-Cy5. A new fluorescent antibody label for three-color flow cytometry with single laser. *Ann NY Acad Sci* 677:185–193, 1993.
116. Wang GT, Chung CC, Holzman TF, Kraft GA: A continuous fluorescence assay of renin activity. *Anal Biochem* 210:351–359, 1993.
117. Wang W, Liang TC: Fluorogenic peptides containing only  $\alpha$ -amino acids. *Biochem Biophys Res Commun* 201:835–840, 1994.
118. Wang Y, Hung S-C, Linn JF, Steiner G, Glazer AN, Sidransky D, Mathies RA: Microsatellite-based cancer detection using capillary array electrophoresis and energy-transfer fluorescent primers. *Electrophoresis* 18:1742–1749, 1997.
119. Wang Y, Ju J, Carpenter BA, Atherton JM, Sensabaugh GF, Mathies RA: Rapid sizing of short tandem repeat alleles using capillary array electrophoresis and energy-transfer fluorescent primers. *Anal Biochem* 67:1197–1203, 1995.
120. Wang Y, Wallin JM, Ju J, Sensabaugh GF, Mathies RA: High-resolution capillary array electrophoretic sizing of multiplexed short tandem repeat loci using energy-transfer fluorescent primers. *Electrophoresis* 17:1485–1490, 1996.
121. Wei A-P, Blumenthal DK, Herron JN: Antibody-mediated fluorescence enhancement based on shifting the intramolecular dimer  $\rightleftharpoons$  monomer equilibrium of fluorescent dyes. *Anal Chem* 66:1500–1506, 1994.
122. Wittwer CT, Herrmann MG, Moss AA, Rasmussen RP: Continuous fluorescence monitoring of rapid cycle DNA amplification. *BioTechniques* 22:130–138, 1997.
123. Wittwer CT, Ririe KM, Andrew RV, David DA, Gundry RA, Balis UJ: The LightCycler: A microvolume multisample fluorimeter with rapid temperature control. *BioTechniques* 22:176–181, 1997.
124. Wolber PK, Hudson BS: An analytic solution to the Förster energy transfer problem in two dimensions. *Biophys J* 28:197–210, 1979.
125. Woolley AT, Mathies RA: Ultra-high-speed DNA sequencing using capillary electrophoresis chips. *Anal Biochem* 67:3676–3680, 1995.
126. Worth RG, Mayo-Bond L, van de Winkel JGJ, Todd FR, Petty HR: CR3 ( $\alpha_M\beta_2$ : CD11b/CD18) restores IgG-dependent phagocytosis in transfectants expressing a phagocytosis-defective Fc $\gamma$ RIIA (CD32): tail-minus mutant. *J Immunol* 157:5660–5665, 1996.
127. Wu P, Brand L: Resonance energy transfer: Methods and applications. *Anal Biochem* 218:1–13, 1994.
128. Youn HJ, Terpetschnig E, Szmecinski H, Lakowicz JR: Fluorescence energy transfer immunoassay based on a long-lifetime luminescent metal-ligand complex. *Anal Biochem* 232:24–30, 1995.
129. Zarewych DM, Kindzelskii AL, Todd RF, Petty HR: LPS induces CD14 association with complement receptor type 3, which is reversed by neutrophil adhesion. *J Immunol* 156:430–433, 1996.
130. Zelenko O, Neumann U, Brill W, Pieleus U, Moser HE, Hosteenge J: A novel fluorogenic substrate for ribonucleases. Synthesis and enzymatic characterization. *Nucleic Acid Res* 22:2731–2739, 1994.
131. Zheng Y, Shopes B, Holowka D, Baird B: Conformations of IgE bound to its receptor Fc $\epsilon$ RI and in solution. *Biochemistry* 30:9125–9132, 1991.
132. Zhou MJ, Poo H, Todd III RF, Petty HR: Surface-bound immune complexes trigger transmembrane proximity between complement receptor type 3 and the neutrophil's cortical microfilaments. *J Immunol* 148:3550–3553, 1992.